



cy.1

ANOMALOUS BEHAVIOR IN THE KINETICS OF PHASE TRANSFORMATION IN CsCl-KCl SYSTEM

K. H. Lin
D. N. Braski

OAK RIDGE NATIONAL LABORATORY
CENTRAL RESEARCH LIBRARY
DOCUMENT COLLECTION
LIBRARY LOAN COPY
DO NOT TRANSFER TO ANOTHER PERSON
If you wish someone else to see this
document, send in name with document
and the library will arrange a loan.

UCN-7969
(3 3-67)



OAK RIDGE NATIONAL LABORATORY
OPERATED BY UNION CARBIDE CORPORATION • FOR THE U.S. ATOMIC ENERGY COMMISSION

Printed in the United States of America. Available from
National Technical Information Service
U.S. Department of Commerce
5285 Port Royal Road, Springfield, Virginia 22151
Price: Printed Copy \$4.00; Microfiche \$0.95

This report was prepared as an account of work sponsored by the United States Government. Neither the United States nor the United States Atomic Energy Commission, nor any of their employees, nor any of their contractors, subcontractors, or their employees, makes any warranty, express or implied, or assumes any legal liability or responsibility for the accuracy, completeness or usefulness of any information, apparatus, product or process disclosed, or represents that its use would not infringe privately owned rights.

ORNL-4872
UC-23 - Radioisotope and
Radiation Applications

Contract No. W-7405-eng-26

ISOTOPES DEVELOPMENT CENTER

ANOMALOUS BEHAVIOR IN THE KINETICS OF
PHASE TRANSFORMATION IN CsCl-KCl SYSTEM

K. H. Lin

D. N. Braski

Isotopes Division

MAY 1973

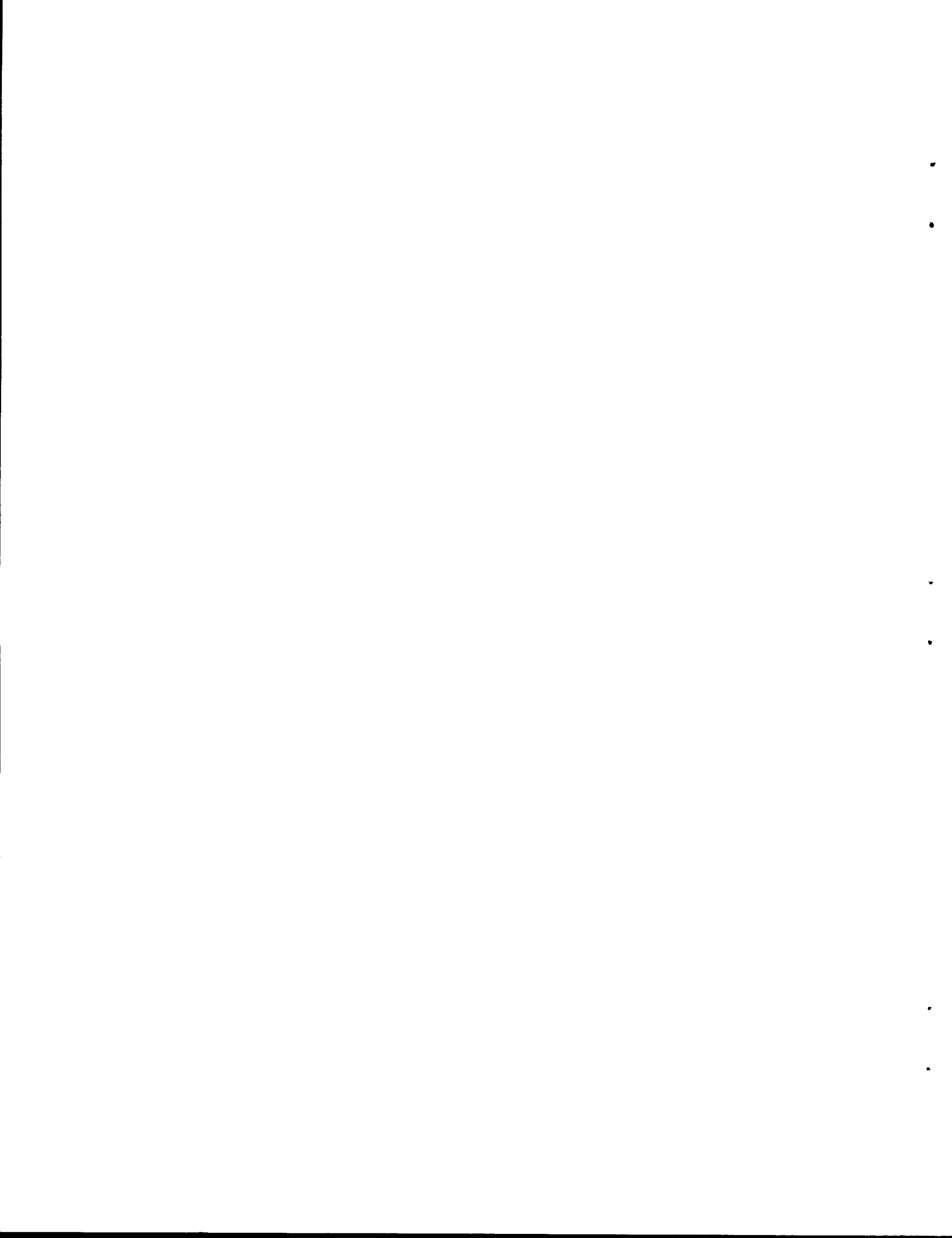
OAK RIDGE NATIONAL LABORATORY
Oak Ridge, Tennessee 37830
operated by
UNION CARBIDE CORPORATION
for the
U.S. ATOMIC ENERGY COMMISSION



3 4456 0050146 4



| CONTENTS | | <u>Page</u> |
|--|--|-------------|
| ABSTRACT | | 1 |
| INTRODUCTION | | 2 |
| EXPERIMENTAL | | 2 |
| I. Materials | | 2 |
| II. Apparatus and Procedure | | 3 |
| A. Differential Thermal Analysis | | 3 |
| B. High-Temperature X-Ray Diffraction | | 3 |
| C. High-Temperature Optical Microscopy | | 5 |
| D. Thermal Expansion Measurement | | 5 |
| E. Kinetics of Transformation | | 6 |
| RESULTS AND DISCUSSION | | 7 |
| I. Differential Thermal Analysis | | 7 |
| II. High-Temperature X-Ray Diffraction | | 10 |
| III. High-Temperature Optical Microscopy | | 12 |
| A. 2 Mole % KCl-CsCl | | 12 |
| B. 20 Mole % KCl-CsCl | | 14 |
| C. 30 Mole % KCl-CsCl | | 15 |
| D. 70 and 80 Mole % KCl-CsCl | | 15 |
| IV. Thermal Expansion | | 19 |
| A. Residual Expansion | | 19 |
| B. Thermal Expansion Coefficient | | 21 |
| V. Phase Diagram of CsCl-KCl System | | 22 |
| VI. Kinetics of Solid-Phase Transformation | | 25 |
| A. The $\beta_1 \rightarrow \alpha + \beta_2$ Phase Transformation in "Dry" Atmosphere | | 26 |
| B. The $\beta_1 \rightarrow \alpha + \beta_2$ Phase Transformation in Air | | 26 |
| C. Observation Under Optical Microscope | | 29 |
| VII. Assessment of Consolidated Results | | 31 |
| A. Role of KCl | | 31 |
| B. Effect of Moisture | | 33 |
| C. Temperature Effect | | 33 |
| CONCLUSIONS AND RECOMMENDATIONS | | 36 |
| REFERENCES | | 38 |



ANOMALOUS BEHAVIOR IN THE KINETICS OF
PHASE TRANSFORMATION IN CsCl-KCl SYSTEM

K. H. Lin and D. N. Braski*

ABSTRACT

The irregular and complex behavior of the CsCl-KCl system in the solid-phase transformation has been investigated using several different techniques including differential thermal analysis (DTA), high-temperature metallography and x-ray diffraction analysis, and dilatometry. Emphasis was placed on CsCl-KCl mixtures having low KCl contents. The DTA results were somewhat misleading in that the solid-phase transformation peak was absent from the thermogram for mixtures containing more than 2 mole % of KCl. Other techniques, however, showed evidences of the structural transformation which varied with the temperature and composition. This variation in the structure was represented by a new phase diagram containing a monotectoid system in the solid-phase region.

In the low KCl range (0-3.2 wt % or 0-7 mole %), the transformation from the low-temperature CsCl structure to the high-temperature NaCl structure was accompanied by a sudden increase in the volume and in the coefficient of linear thermal expansion. There was a tendency for the low KCl-CsCl mixture (including pure CsCl) to retain and accumulate significant portions of residual expansion at room temperature when the mixture was subjected to thermal cycling through the solid-phase transformation temperature. This problem was most serious with pure CsCl. Such behavior could lead to rupture of the $^{137}\text{CsCl}$ gamma source capsule if not properly designed.

The kinetics and mechanism of the solid-phase transformation in the cooling step are governed most remarkably by the moisture in the gaseous atmosphere, and to a lesser extent by the composition and temperature. The extremely slow solid-phase transformation on cooling in a dry atmosphere ($\sim 2 \times 10^{-3}$ Torr) was demonstrated by the 20 mole % KCl-CsCl mixture in which approximately 40% of the high-temperature (NaCl) structure was retained at room temperature even after 600 hr. In contrast, exposure of the same mixture to air (40% relative humidity) upon cooling to room temperature completed the transformation within 20 sec.

*Presently a member of the Chemical Technology Division.

INTRODUCTION

With the development of the nuclear power industry in recent years, nuclear fission products have been receiving close attention because their impact on the environment depends upon the methods of disposition. One potentially useful fission product is an isotope of cesium with a mass of 137, having a long half-life (30 years) and relatively high radiation energy levels from negative beta particles and gamma rays. Cesium chloride has been the preferred and accepted gamma source compound based on ^{137}Cs .

In spite of many desirable properties, CsCl has one disadvantage in that it undergoes solid-phase transformation at approximately 460°C , resulting in a sudden expansion in volume. Such a property presents problems in the design of capsules for the $^{137}\text{CsCl}$ source, because a sufficient volume must be allowed for expansion caused by the phase transformation. Since KCl may be one of the major impurities in $^{137}\text{CsCl}$, its effects on the phase behavior and other physical properties of CsCl must be determined.

The limited number of phase diagrams for CsCl-KCl system available in the literature¹⁻⁴ cover only the liquidus and solidus curves; behavior in the solid phase region has never been published. Furthermore, some disagreement exists in the liquidus and solidus among different investigators. In the practical application of a $^{137}\text{CsCl}$ gamma source, the temperature should never approach the melting point. Accordingly, knowledge of the solid-phase behavior of the CsCl-KCl system is of great importance in capsule design and final application of the $^{137}\text{CsCl}$ source. Preliminary data from differential thermal analysis (DTA) revealed a complex behavior of the system, particularly for mixtures of low KCl content for which the solid-phase transformation peak of pure CsCl on the DTA thermogram was no longer visible in the heating step. On the other hand, there were peaks on cooling, indicating some types of solid-phase transformation, but the transformation was quite sluggish. Such anomalous behavior has never been reported previously for the CsCl-KCl system.

In view of the problems mentioned above, the objectives and scope of the present investigation are: (1) to elucidate the complex behavior of the CsCl-KCl system in the solid-phase region with emphasis on the significance of disappearance of the DTA peaks for mixtures having low KCl contents, and (2) to prepare the phase diagram for the CsCl-KCl system based on data from different techniques including DTA, high-temperature x-ray diffraction, dilatometry, and high-temperature photomicrography.

EXPERIMENTAL

I. Materials

Chemicals used in the present study were reagent-grade KCl (99.8% purity, Baker Chemical Company) and high-purity CsCl (99.95% pure, Kawecki Berylco Industries, Inc.). Both compounds were dried at 150°C before use. The

CsCl-KCl mixtures of various composition were prepared by thoroughly blending proper amounts of individual salts in a small ball mill. Some mixtures were also prepared by solvent evaporation and cocrystallization of aqueous solutions containing desired proportions of KCl and CsCl. The homogeneity of each mixture and absence of impurities which might have been introduced during mixing were ensured by chemical analysis of samples taken from several different locations. Potassium chloride of very high purity (100.0%, Baker Chemical Company) was also used in several DTA runs (alone and in the CsCl-KCl mixtures). An excellent agreement in the DTA thermograms was obtained between the runs using the reagent-grade KCl and those using the very high purity KCl.

II. Apparatus and Procedure

A. Differential Thermal Analysis

The key components in the differential thermal analyzer (DuPont 900 Differential Thermal Analyzer) included an intermediate temperature DTA cell capable of operation up to 850°C, a temperature programmer-controller, and an X-Y recorder. The recorder plots the sample temperature on the X-axis and the differential temperature between the reference material (alumina) and the sample on the Y-axis. Contained in the cell are a cartridge heater centrally located in a cylindrical silver block which accommodates a control thermocouple, and two quartz tubes (2- or 4-mm ID) with thermocouples, one for the sample and the other for the reference material.

Each of the CsCl-KCl samples of various compositions (0-100% KCl; prepared by the method described in the preceding section) was introduced into the sample tube, the thermocouple carefully centered in the sample, and the DTA cell assembled. After alternately evacuating the DTA cell and purging with helium gas at least three times, the run was started by heating the cell at a predetermined rate (5-20°C/min), and the thermogram recorded on the calibrated X-Y recorder. Upon reaching the melting point, the heater was turned off, and the sample was cooled to room temperature with continued recording of the thermogram. A slight flow of helium gas was maintained throughout the run. The same sample was subjected to at least two additional heating-cooling cycles by repeating the above procedure. Only thermograms obtained from the second cycle and thereafter were considered in the data analysis. The DTA apparatus was adjusted by determining thermograms for individual compounds and comparing them with the literature data. Several pure compounds, including CsCl and KCl, were used.

B. High-Temperature X-Ray Diffraction

The x-ray diffraction unit used in this investigation was a Siemens horizontal diffractometer with a graphite monochromator on the diffracted beam. The copper target x-ray tube was operated at 35 kV and 20 mA with an entrance slit of 2° and a receiver slit of 0.2 mm. The KCl-CsCl powder mixtures were heated in an x-ray hot stage (Materials Research

Corporation) mounted on the diffractometer. The stage consisted of an aluminum body and two water-cooled terminals for electrical resistance heating of the sample. The aluminum cover had a thin beryllium window to permit transmission of the x-ray beam and to seal the specimen in an air-tight chamber. The hot stage was operated with the chamber either filled with air or argon or under a vacuum.

The type of x-ray specimen furnace used to heat the sample was fabricated from 1.27- by 3.82-cm tantalum strips having a nominal thickness of 0.076 mm. The strips were bent in dies so that the center portion of the element formed a rectangular boat. An even layer of sample powder was placed in the boat and then covered with a 0.25-mm-thick beryllium cover window. The two ends of the tantalum boat were crimped over to hold the beryllium window in place. With this design it was possible to heat a thin powder wafer to melting and still contain it in the vertical position necessary for x-ray analysis. A Chromel-Alumel thermocouple spot-welded to the back of the boat was used to monitor the sample temperature.

The first step in conducting an x-ray diffraction run was to melt the KCl-CsCl powder mixture. This was accomplished by heating the sample in the hot stage at a rate of approximately 20°C/min under a stream of argon (slightly above 1 atm) to the melting point. Melting of the sample was characterized by a rapid disappearance of its x-ray diffraction peaks. This procedure was carried out twice before data were taken to ensure that melting was complete. On the third cycle the sample was again heated at approximately 20°C/min and x-ray diffraction patterns were taken at 100°C intervals. Before taking an x-ray pattern the sample was always allowed to reach an equilibrium temperature for about 10 min.

Upon approaching the melting point, the sample was subsequently cooled at approximately 20°C/min and x-ray patterns were obtained at approximately 100°C intervals until room temperature was reached. In the fourth cycle, patterns were taken at smaller temperature intervals near the phase transformation point as indicated by the previous run. A single x-ray diffraction peak of the transforming phase (low-temperature structure) was monitored in a fifth cycle as the sample was slowly heated through the transformation temperature. The beginning of the solid-phase transformation was characterized by a decrease in the x-ray intensity and was essentially complete when the diffraction peak disappeared. Sometimes samples were run under vacuum instead of argon to enhance the resolution of the diffraction pattern. Analysis under vacuum ($\sim 10^{-3}$ Torr pressure) always produced an increase in the diffracted intensity by a factor of 2 or 3. However, the sample was never heated above 500°C under vacuum in order to minimize vaporization of the halides. The x-ray patterns were always obtained over a 2θ angular range of 20-32°. This range was particularly convenient because it contained two major peaks for each of the three solid phases in the KCl-CsCl system. It was also advantageous in that no diffraction peaks from the beryllium window or tantalum heater were in that range. Analysis would have been very difficult above 32° because many of the beryllium and tantalum peaks were superimposed over the halide peaks.

C. High-Temperature Optical Microscopy

The optical microscope (E. Leitz Company Orthoplan), which was equipped with a high-temperature stage (Leitz Microscope Heating Stage 1350) (1350°C maximum) and photographic accessories, was capable of examining the sample under either transmitted light or incident light. The stage was provided with a water-cooled jacket and a gas-tight seal that made observation in an inert gas atmosphere possible. Sample temperature during examination was recorded on the strip-chart recorder, and the high-temperature stage was calibrated with a set of melting point standard materials including analytical reagents of benzoic acid, $K_2Cr_2O_7$, $Ba(NO_3)_2$ and LiF, and high-purity silver, gold, and copper.

The stage containing the sample was gradually heated in an argon atmosphere to the melting point, after which cooling of the stage proceeded slowly to room temperature. Such a heating-cooling cycle was repeated at least twice during which photomicrographs of the sample were recorded whenever any significant change took place. The photomicrographs served as the supplement to the data from the DTA and the high-temperature x-ray diffraction analysis in the interpretation of the CsCl-KCl phase diagram.

D. Thermal Expansion Measurement

The equipment (Brinkmann-Netzsch Dilatomer) employed in the thermal expansion study consisted of the dilatometer measuring system, the tube furnace (up to 1550°C), and the control cabinet. The control cabinet contained a power supply, a temperature programmer, and a two-pen strip-chart recorder that simultaneously recorded the expansion (or contraction) (maximum linear range ± 0.08 in.) and temperature (0-1000°C) with an accuracy of 0.5%. Cylindrical pellets were prepared from CsCl-KCl mixtures (mechanical and molten) of three different compositions (0, 2, and 7 mole % KCl). All the pellets were approximately 0.5 in. in diameter and 1 in. long, with the density in excess of 97% of the theoretical value (i.e., 0% void volume).

Prior to the measurement of thermal expansion for the CsCl-KCl pellets, the dilatometer was calibrated by using the standard fused quartz cylinder (~ 0.5 -in. diameter and 2 in. long) to obtain the correction curve to account for the expansion of the measuring system. The calibration was carried out by simultaneously recording the temperature and the amount of linear thermal expansion under a preset heating rate (10°C/min) up to 1200°C, followed by cooling to room temperature. The thermal expansion curve (as in./in.) of the measuring system containing the quartz standard calculated from the data recorded on the chart was compared with the literature data for expansion of quartz to establish the correction curve.

Thermal expansion measurements for the CsCl-KCl pellets were made by the procedure similar to that for the quartz standard in the calibration, except that the upper temperature was limited to 550°C. Expansion data recorded on the chart were subsequently corrected based on the calibration curve established above.

E. Kinetics of Transformation

The 20 mole % KCl-CsCl mixture was selected for this study. The high-temperature x-ray diffraction unit, described previously, (Section II.B) was the major piece of equipment used in the kinetic study of structural transformation of the CsCl-KCl solid solution. The basic procedure for the use of the x-ray unit was the same as before. To investigate the kinetics of transformation as a function of temperature, an additional step termed "isothermal annealing" was adapted. In this step, the molten KCl-CsCl mixture was cooled to and maintained at a specified temperature while the phase transformation was monitored by the x-ray unit.

The experimental run started with heating of the KCl-CsCl mixture at a rate of approximately 20°C/min to the melting point in the high-temperature stage under a flow of argon, such that the gas pressure in the stage was slightly above 760 Torr. The melt was then cooled immediately at the same rate to room temperature and was subsequently exposed to air (~40% relative humidity). The stage, after evacuation to 2×10^{-3} Torr, was refilled with argon gas before resuming the melting step. Such a heating-cooling cycle was repeated at least twice before subjecting the sample to the isothermal annealing treatment. In one series of experiments, isothermal annealing was carried out under vacuum ($\sim 2 \times 10^{-3}$ Torr). In contrast, the sample was exposed to ambient air of approximately 40% relative humidity during the isothermal annealing in the other series of experiments.

In either series of experiments, the amount of β_1 phase* retained under isothermal conditions was monitored by x-ray diffraction as a function of time. Monitoring was facilitated by the use of the Siemens card programmer to step-scan over the β_1 (200) peak in 0.05 degree (2θ) increments. The step-scan was performed at predetermined time intervals until the $\beta_1 \rightarrow \alpha + \beta_2$ transformation* was practically complete. The areas under the β_1 (200) peaks were then determined by means of a planimeter from the plot of the scans. The "single-line" technique for quantitative analysis by x-ray diffraction⁵ was utilized to correlate the area or intensity of the β_1 (200) reflection to its weight fraction in the sample as follows:

$$W_{\beta_1} = I_{\beta_1} / (I_{\beta_1})_p$$

where

$$\begin{aligned} I_{\beta_1} &= \text{intensity of } \beta_1 \text{ (200) reflection from KCl-CsCl mixture} \\ (I_{\beta_1})_p &= \text{intensity of } \beta_1 \text{ (200) reflection from sample containing} \\ &\quad \text{pure } \beta_1 \text{ phase} \\ W_{\beta_1} &= \text{weight fraction of } \beta_1 \text{ in the mixture} \end{aligned}$$

This technique was applicable because the mass absorption coefficients of the β_1 phase and its transformation product phases ($\alpha + \beta_2$) were identical.

*The α phase is a solid solution of KCl in CsCl having the CsCl structure. The β_1 and β_2 phases are solid solutions of CsCl and KCl having the NaCl structure. The β_1 phase is rich in CsCl whereas the β_2 phase contains mostly KCl. The two phases have different lattice parameters.

RESULTS AND DISCUSSION

I. Differential Thermal Analysis

Listed in Table 1 are the solidus and liquidus temperatures at various compositions of the CsCl-KCl system as determined from the DTA thermograms. Also shown are temperatures at which the solid-phase transformation took place from the low-temperature structure (CsCl) to the high-temperature structure (NaCl). The data in Table 1 are based on the heating curves of the DTA thermograms and were mostly reproducible to within $\pm 2^\circ\text{C}$. The cooling curves were not used, since the solid-phase transformation of the

Table 1. Differential Thermal Analysis Data for CsCl-KCl System

| Composition (mole %) | | Temperature ($^\circ\text{C}$) | | |
|-------------------------|-------|----------------------------------|----------|-------------------------------|
| CsCl | KCl | Solidus | Liquidus | Solid-Phase Transformation |
| 100.0 | 0.0 | 639 | 639 | 464 |
| 99.0 | 1.0 | 634 | 637 | 461 |
| 98.5 | 1.5 | 631 | 636 | 462 |
| 98.0 | 2.0 | 631 | 638 | |
| 97.0 | 3.0 | 626 | 634 | |
| 96.0 | 4.0 | 626 | 630 | |
| 95.0 | 5.0 | 620 | 635 | |
| 93.0 | 7.0 | 620 | 627 | |
| 90.0 | 10.0 | 612 | 623 | |
| 85.0 | 15.0 | 606 | 616 | |
| 80.0 | 20.0 | 601 | 611 | |
| 75.0 | 25.0 | 599 | 608 | |
| 70.0 | 30.0 | 596 | 605 | |
| 65.0 | 35.0 | 596 | 600 | |
| 60.0 | 40.0 | 597 | 602 | |
| 55.0 | 45.0 | 598 | 605 | |
| 50.0 | 50.0 | 598 | 606 | |
| 30.0 | 70.0 | 642 | 670 | |
| 20.0 | 80.0 | 671 | 704 | |
| 10.0 | 90.0 | 710 | 734 | |
| 5.0 | 95.0 | 725 | 752 | |
| 0.0 | 100.0 | 767 | 767 | |

CsCl-KCl system on cooling was extremely sluggish and was not reproducible. Selected DTA thermograms are presented in Figs. 1-5 to illustrate the anomalous behavior of the system in the thermal differential analysis.

According to Table 1, no solid-phase transformation could be detected on the DTA thermogram (heating curve) for mixtures with a KCl content of 2 mole % or higher. The diminishing and subsequent disappearance of the solid-phase transition peaks (on a DTA thermogram) with increasing KCl content in the CsCl-KCl system is also demonstrated in Figs. 1-5. Thus, for pure CsCl the solid-phase transition peak on heating appears at 464°C. On cooling, the solid-phase transformation temperature is depressed appreciably, indicating a significant hysteresis effect. This hysteresis effect becomes more pronounced as a small amount (1 mole %) of KCl is added to CsCl (Fig. 2). At the same time, the heights of the solid-phase transformation peaks are reduced considerably (the ΔT scale of Fig. 2 is twice that of Fig. 1). When the KCl content is increased to 2 mole % (Fig. 3), the solid-phase transformation peak is no longer observed on heating, but a "blip-like" peak appears on cooling — the location and height of which were not reproducible — although the temperature of this peak is always far below that of pure CsCl. With the mixture containing 7 mole % KCl (Fig. 4), the blip that appears on cooling is shifted to a lower temperature than that observed with the 2 mole % KCl-CsCl mixture. Finally, when the KCl content reaches 15 mole % (Fig. 5), the blip disappears completely.

The disappearance of the solid-phase transformation peak on the DTA thermogram discussed above does not represent the true phenomenon taking place in the CsCl-KCl system. That is, the addition of any amount of KCl to CsCl does not eliminate solid-phase transformation (except near 100% KCl), but merely changes the types of solid phases that are determined by the composition and temperature. This statement is based on evidence from high-temperature x-ray diffraction analysis, high-temperature optical microscopy, and dilatometry. (Results from these techniques are discussed elsewhere in this report.)

The peak area on the DTA thermogram is related to the heat of transformation. Since the solid-phase transformation took place rapidly on heating, as observed by other techniques (high-temperature x-ray diffraction and optical microscopy), the disappearance of the peak in the heating step probably implies that the heat of (solid phase) transformation of CsCl had been reduced drastically as the result of the KCl addition. A similar statement is applicable to cooling of CsCl-KCl mixtures with high KCl contents (greater than 25-30 mole %). On the other hand, the absence of peaks on cooling the mixtures containing approximately 15-20 mole % KCl represents sluggishness in transformation; in a dry inert atmosphere, the major portion of the unstable high-temperature NaCl structure was retained for extended periods of time even at room temperature. With mixtures of lower KCl contents (2-10 mole %), the blips that appear on cooling probably indicate partial transformation of the NaCl structure to the CsCl structure as supported by the x-ray data and photomicrographs. Thus, the behavior of the CsCl-KCl system is quite complex, especially in the cooling step, and the details on the kinetics and mechanism of such behavior are discussed elsewhere in this report.

ORNL DWG. 73-2472

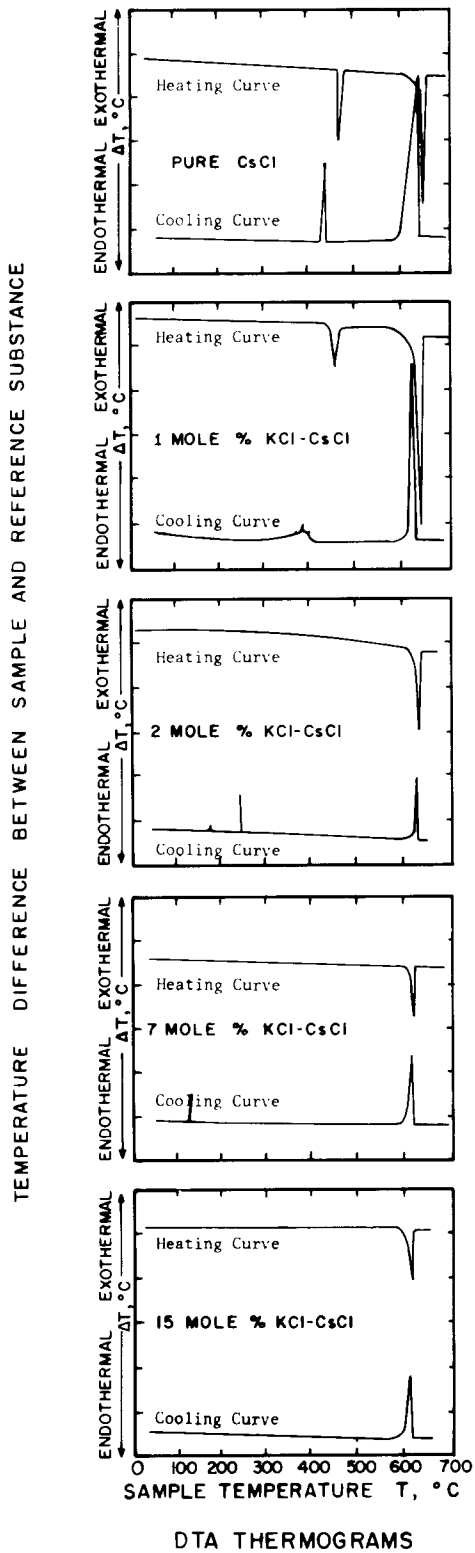


Fig. 1. Pure CsCl.

Fig. 2. 1 Mole % KCl-CsCl.

Fig. 3. 2 Mole % KCl-CsCl.

Fig. 4. 7 Mole % KCl-CsCl.

Fig. 5. 15 Mole % KCl-CsCl.

II. High-Temperature X-Ray Diffraction

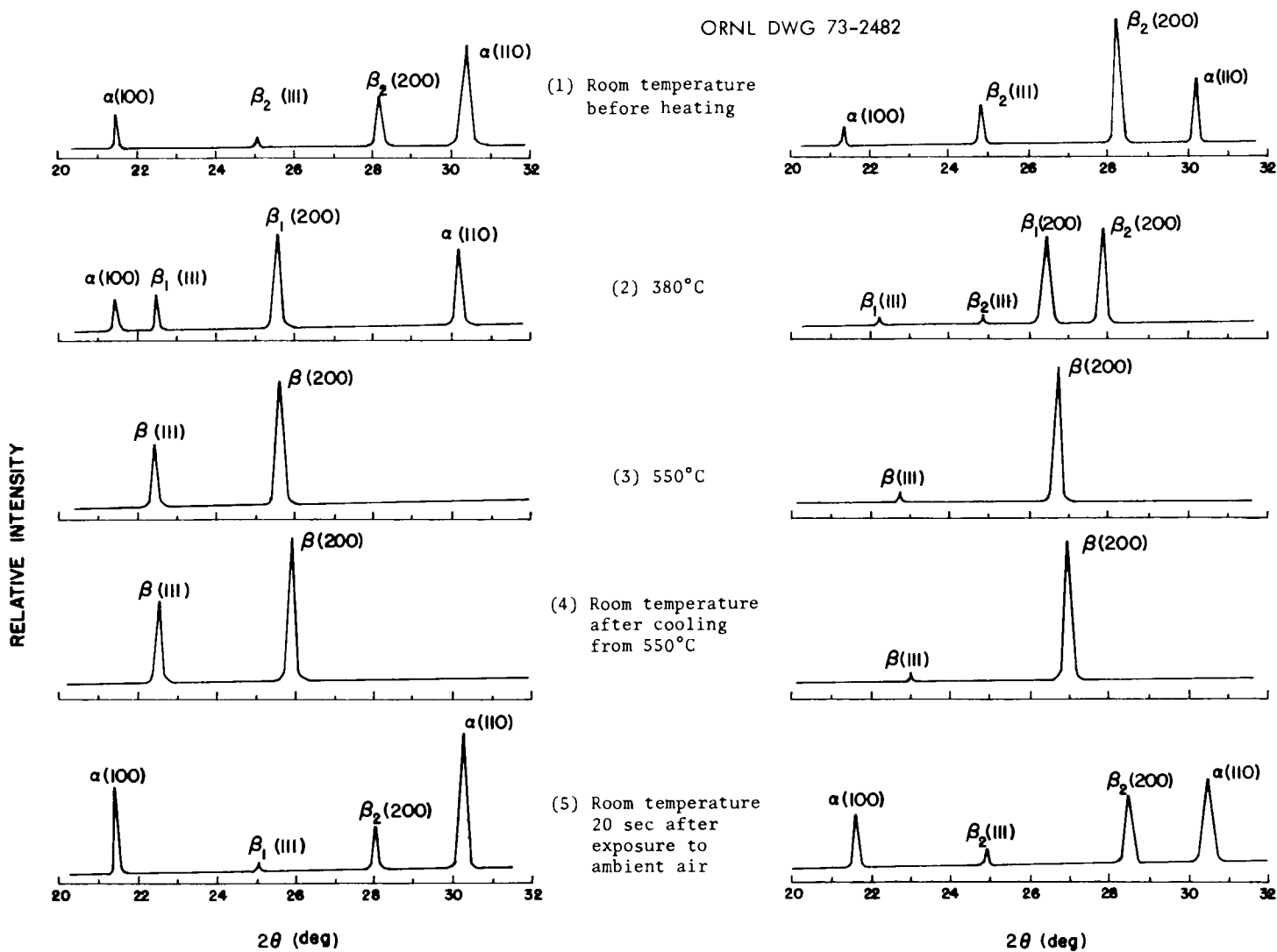
The anomalous behavior of the KCl-CsCl system in the solid-phase region in the differential thermal analysis was clarified by x-ray diffraction analysis at high temperatures. The typical phase transformation of the system can be illustrated by referring to Fig. 6, which shows selected x-ray diffraction patterns for mixtures containing 20 and 70 mole % KCl (Figs. 6A and 6B, respectively). Both mixtures have previously been molten and cooled to room temperature (Figs. 6A-1 and 6B-1). In either case, two phases are present at room temperature: an α -phase solid solution of KCl dissolved in CsCl with the CsCl structure, and a β_2 -phase solid solution of CsCl dissolved in KCl with a rock salt structure. The lattice parameter of β_2 -phase is essentially that of pure KCl indicating that the amount of CsCl dissolved in β_2 -phase solid solution was very small.

When the 20 mole % KCl-CsCl mixture was heated above 360°C (Fig. 6A-2) the structure consisted of α -phase and β_1 -phase. The β_1 -phase has the same rock salt structure as β_2 , but differs in the composition (β_1 is rich in CsCl while β_2 is rich in KCl) and lattice parameter. Therefore the β_1 -phase must have been formed by the reaction of a portion of α -phase (rich in CsCl) with β_2 -phase (rich in KCl), the resulting product assuming the rock salt structure. Further heating of the α - and β_1 -phases (Fig. 6A-3) to 550°C produced an all β structure.* Subsequent cooling to room temperature (Fig. 6A-4) (either in the dry argon atmosphere or under vacuum) did not produce a transformation; the same structure was retained. The only difference between the x-ray diffraction pattern at 550°C (Fig. 6A-3) and this one taken after cooling to room temperature is a slight shift of the peaks which reflects the effect of thermal contraction of the crystal lattice. However, when ambient air was allowed into the high-temperature stage chamber, transformation to the stable $\alpha + \beta_2$ phase occurred within 20 seconds. This unusual phase transformation is believed to be moisture sensitive and is discussed in some detail elsewhere in this paper (see Kinetics of Solid-Phase Transformation). The discovery of the moisture sensitivity of the $\beta_1 \rightarrow \alpha + \beta_2$ phase transformation explains why the DTA analysis was unable to detect it. Since the DTA samples were in a dry environment after cooling, the β -phase structure was retained, and no phase transformation took place upon subsequent heating. The influence of moisture on the transformation could be the reason that early investigators did not observe the solid-state phase fields on the KCl-CsCl phase diagram.

Figure 6B shows similar x-ray diffraction patterns for the 70 mole % KCl-CsCl mixture. At room temperature (Fig. 6B-1) the structure is likewise a mixture of α - and β_2 -phases. At 380°C (Fig. 6B-2) all of the α -phase has transformed to β_1 -phase, and the resultant structure consists of both β_1 - and β_2 -phases. At 550°C (Fig. 6B-3) a single β -phase exists whose composition and lattice parameter are between those of the β_1 - and β_2 -phases from which it was formed. Again the β -phase was retained on cooling to room temperature (Fig. 6B-4) and transformed rapidly to the stable

*A "β" designation is used to define the single solid solution of CsCl and KCl having the NaCl structure at high temperatures.

ORNL DWG 73-2482



[A] 20 mol % KCl-CsCl

[B] 70 mol % KCl-CsCl

Fig. 6. X-Ray Diffraction Patterns [In argon atmosphere except (5)].

$\alpha + \beta_2$ phases upon exposure to ambient air (Fig. 6B-5). From the results just described, it is obvious that: (1) x-ray analysis of KCl-CsCl samples for phase diagram determination should include a short exposure to air before reheating in a dry, inert environment, and (2) the determination of solid-state transformation temperatures should be made on heating rather than cooling the sample.

III. High-Temperature Optical Microscopy

Photomicrographs of selected samples were taken at various temperatures to obtain visual qualitative evidences of different types of phase transformation. Most of the photomicrographs were taken by means of transmitted light, but reflected light was also used in some instances. In both cases, the light intensity was maintained constant. One of the outstanding characteristics noted during microscopic examination of samples was the light-absorbing property of different solid phases. That is, the α -phase has the highest "light absorptivity" followed by the β_1 - and β_2 -phases. No attempt was made to quantitatively determine the light absorptivity of these phases, but the difference in the brightness of optical images between the α - and β -phases was quite distinct. This and other pertinent observations are discussed for samples containing 2, 20, 30, 70, and 80 mole % KCl.

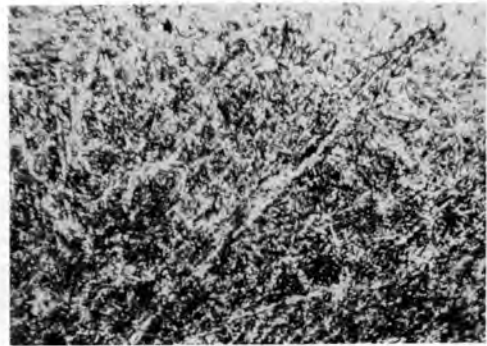
A. 2 Mole % KCl-CsCl

Illustrated in Fig. 7 are photomicrographs of the 2 mole % KCl-CsCl mixture at various temperatures. Figure 7a shows the premolten mixture at room temperature, which is known to be of the CsCl structure (α -phase). Heating in an argon atmosphere to 470°C results in an appreciably brighter image (Fig. 7b) indicating that the structure had transformed into the β -phase at this temperature, as revealed by x-ray diffraction. An additional change in the microstructure is observed (Fig. 7c) with further increase in temperature. Depicted in Fig. 7d is the spheroidized structure at 620°C after going through the melting step. This structure persisted during the cooling step until about 210°C when it suddenly (in a fraction of a second) turned dark (Fig. 7e) indicating transformation of the β -phase to the α -phase. The temperature of this transformation was not too reproducible due to the sluggishness in transformation on cooling, but it generally ranged from 200-250°C.

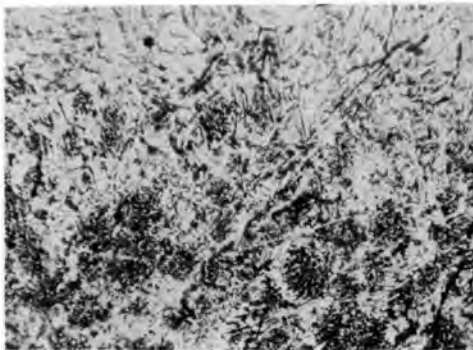
Based on the observation described above, the $\alpha \rightarrow \beta$ phase transformation on heating appeared to take place in an orderly manner and was in sharp contrast with the abrupt $\beta \rightarrow \alpha$ phase transformation on cooling. Such an anomalous behavior of the 2 mole % KCl-CsCl mixture presumably explains the shape of the DTA thermogram (Fig. 3) which exhibits no solid-phase transformation peak on heating, while displaying a large degree of undercooling with a sharp peak (blip) on cooling. One of the features of this mixture as compared to others of high KCl content was formation of irregular-shaped fractures on cooling primarily along grain boundaries (not shown here). Mixtures having high KCl contents (e.g., ≥ 20 mole %) tended to produce regular-shaped (i.e., rectangular and/or square) fractures within grain boundaries (detailed discussion to follow).



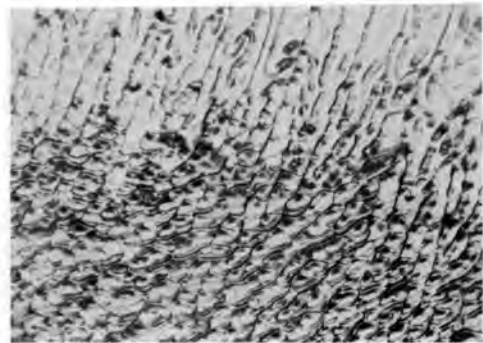
(a) 25°C



(b) 470°C; Heating



(c) 550°C; Heating



(d) 620°C; Cooling after melting

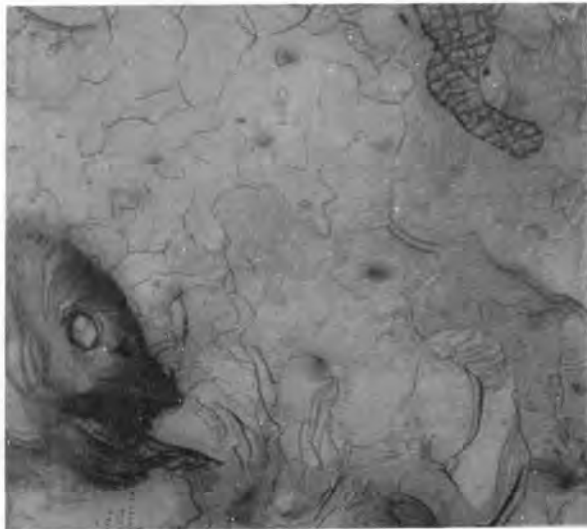


(e) 210°C; Cooling

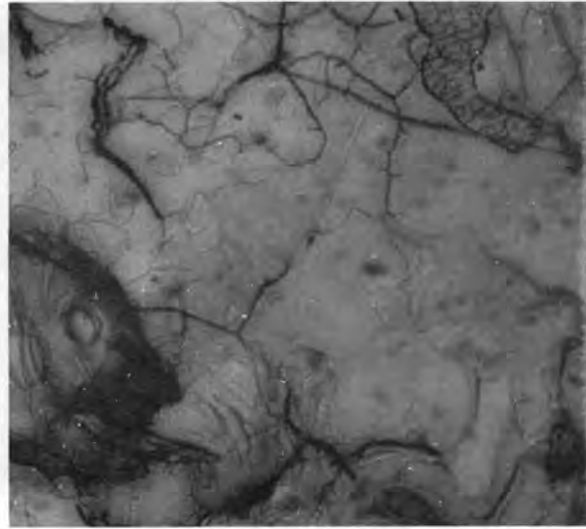
Fig. 7. Microstructure of 2 Mole % KCl-CsCl.
Magnification: 100X; transmitted light.

B. 20 Mole % KCl-CsCl

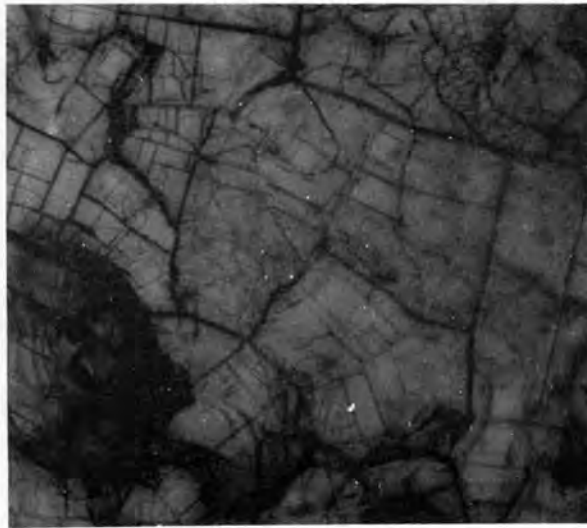
Variation in the microstructure of the 20 mole % KCl-CsCl with temperature is demonstrated in Fig. 8. The sample that was cooled to 575°C from the melt appears to have a relatively smooth surface (Fig. 8a). The dark area near the lower left corner represents the portion having a greater thickness than the remaining area. Cooling to 380°C produces fractures along



(a) 575°C; Reflected polarized light



(b) 380°C; Reflected polarized light



(c) 25°C; Reflected polarized light



(d) 25°C; After exposure to atmosphere; transmitted light

Fig. 8. Microstructure of 20 Mole % KCl-CsCl.
Magnification: 80X; cooling.

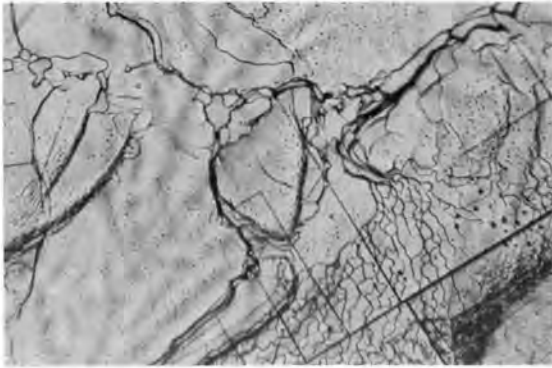
grain boundaries (Fig. 8b) and causes a slight increase in the number of grayish "spots" throughout, possibly indicating the onset of a phase transformation. As the temperature falls further, orderly arranged fractures are found within grain boundaries (Fig. 8c), fractures within the same grain boundary being either parallel to or perpendicular to one another. The contrast in brightness among different portions of the image remains basically the same. Upon exposure to atmosphere (~40% relative humidity), however, distinctly dark areas are distributed in the light background (Fig. 8d). Based on the x-ray diffraction study (Fig. 6), dark areas are presumably the α -phase; whereas, the light areas represent the β_2 -phase. The moisture in the atmosphere apparently accelerates the $\beta \rightarrow \alpha$ phase transformation. The influence of the moisture is also seen in widening of fractures giving grayish fringes along the cracks. The significance of interaction between moisture and the KCl-CsCl mixture is discussed elsewhere in more detail (see Sections VI and VII).

C. 30 Mole % KCl-CsCl

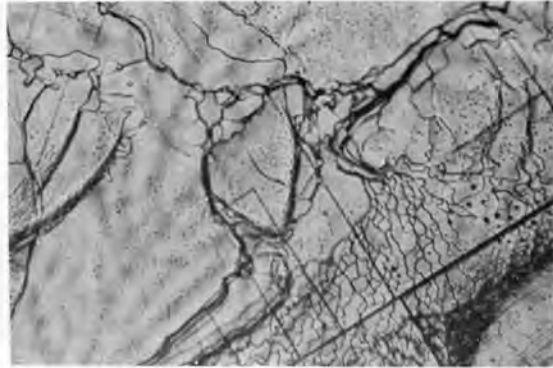
Scattered spheroidal precipitates appeared in the light-colored matrix upon cooling to approximately 360°C (Fig. 9a). The density of these precipitates increased only slightly when cooled to room temperature (Figs. 9b and 9c). Development of rectangular fractures within individual grain boundaries are again observed as the temperature decreased. Exposure of the sample to the environmental atmosphere resulted in the partial transformation of the β -phase to the α -structure (dark area, Fig. 9d), simultaneously broadening the fractured boundary lines. Also, some spheroidal precipitates appeared to be dissolving. Reheating to 380°C produced a lighter colored structure and rendered both the precipitates and the matrix somewhat diffuse in appearance (Fig. 9e). Such effects were amplified as the temperature was raised to 550°C (Fig. 9f), probably suggesting completion of the $\alpha \rightarrow \beta$ transformation.

D. 70 and 80 Mole % KCl-CsCl

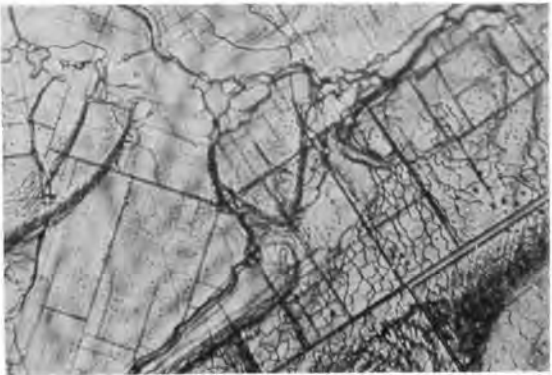
Figure 10a presumably represents a mixture of the CsCl-rich α -phase (darker areas) and the KCl-rich β_2 -phase (lighter areas including those overlapping with the α -phase) at room temperature (refer to the x-ray diffraction pattern in Fig. 6B). In general, the sizes of fractures in this composition are considerably smaller than those of other compositions. Once again, heating through a series of temperatures increased the brightness of the image, indicating progress of the $\alpha \rightarrow \beta$ phase transformation, and caused the fractures to fade away (Figs. 10b and 10c). Similar behavior was observed in the case of 80 mole % KCl-CsCl, but the sizes of grains and fractures were much larger than those of 70 mole % KCl-CsCl (Fig. 11).



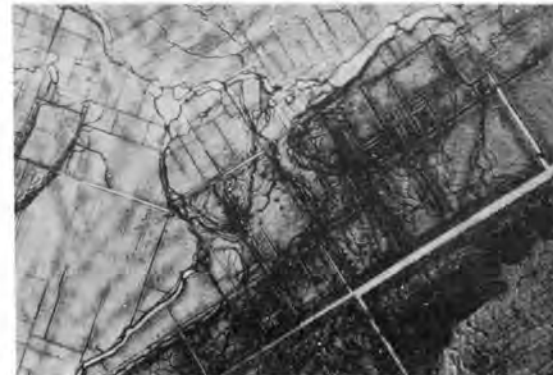
(a) 360°C; Cooling



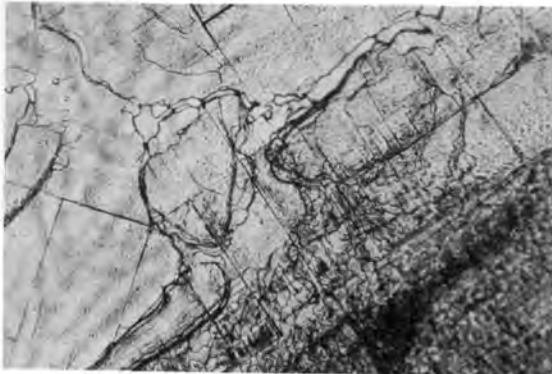
(b) 330°C; Cooling



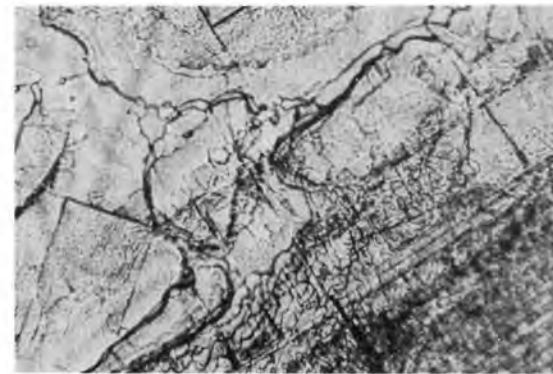
(c) 120°C; Cooling



(d) 30°C; After exposure to atmosphere



(e) 380°C; Heating



(f) 550°C; Heating

Fig. 9. Microstructure of 30 Mole % KCl-CsCl.
Magnification: 100X; transmitted light.



(a) 25°C



(b) 370°C; Heating

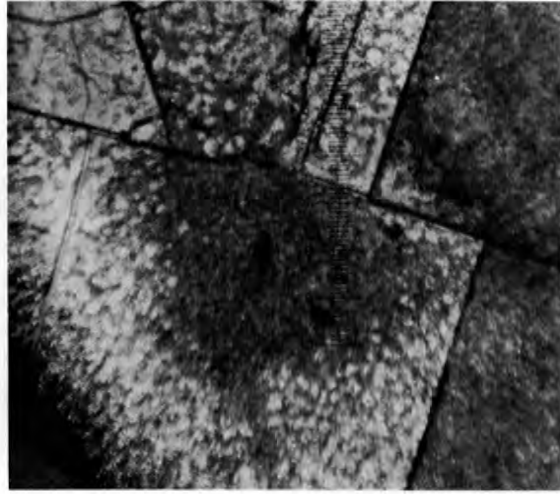


(c) 550°C; Heating

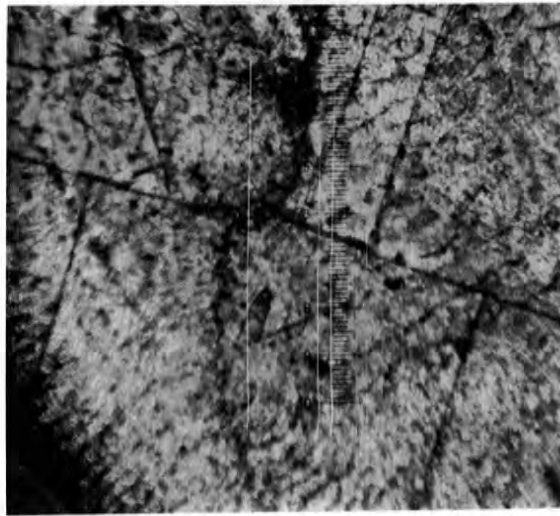
Fig. 10. Microstructure of 70 Mole % KCl-CsCl.
Magnification: 50X; transmitted light.



(a) 240°C; Heating



(b) 450°C; Heating



(c) 630°C; Heating

Fig. 11. Microstructure of 80 Mole % KCl-CsCl.
Magnification: 80X; transmitted light.

IV. Thermal Expansion

Knowledge of the thermal expansion properties of CsCl as well as of CsCl containing impurities (e.g., KCl) is of practical importance in the design of $^{137}\text{CsCl}$ source forms. The linear dimensional changes of cylindrical samples under a programmed variation in temperature up to 550°C were determined for CsCl and CsCl-KCl mixtures (both molten and mechanical; 2 and 7 mole % KCl). Three heating-cooling cycles were carried out for all samples except one to investigate the effect of repeated thermal cycling on their thermal expansion behavior. The outstanding characteristics of these samples observed during dilatometric measurements include (a) the tendency to retain significant amounts of residual expansion at room temperature and (b) the large difference in the thermal expansion coefficients between the pretransformation and posttransformation conditions.

A. Residual Expansion

Presented in Table 2 are the magnitudes of linear expansion (expressed as percent of the length at the start of each heating-cooling cycle) at various temperatures for CsCl and CsCl-KCl mixtures. Both heating and cooling data near the solid-phase transformation are included. Data from Table 2 demonstrate that thermal expansion of CsCl and CsCl-KCl mixtures (2 and 7 mole % KCl) was not completely reversible. The amount of expansion retained by the sample after each thermal cycle varied with the sample type, but in all cases it diminished with repeated cycling. The tendency to retain the residual expansion after cooling to room temperature was most noticeable in pure CsCl (12.9% after two runs based on the length before cycle 1). Addition of a small amount of KCl (e.g., 2 mole %) reduced this tendency considerably; i.e., after two runs the residual expansion is only 5.5% for the molten 2 mole % KCl-CsCl. Retention of the residual expansion in this manner implies that if a $^{137}\text{CsCl}$ gamma source were subjected to repeated thermal cycling through approximately 550°C , a significant amount of stress might develop in the source capsule.

A sudden jump in the percent linear expansion was observed for all samples, generally in the temperature range where the solid-phase transformation of CsCl takes place (464°C). For pure CsCl, there was an abrupt contraction ($>1\%$ of the starting length) between $460\text{-}480^\circ\text{C}$ followed by a sudden expansion. No such behavior was displayed by the 2 mole % KCl-CsCl. When pure CsCl was cooled, the equivalent shift took place in the $450\text{-}400^\circ\text{C}$ range. Such changes in the thermal expansion characteristics were obviously caused by the solid-phase transformation as shown by the DTA thermogram (Fig. 1).

For the 2 mole % KCl-CsCl mixture (mechanical), the sudden jump in the linear expansion also took place between $450\text{-}500^\circ\text{C}$ (except for cycle 1). Cooling of the same mixture resulted in a relatively mild shift in the percent expansion in the $300\text{-}400^\circ\text{C}$ range. The behavior of the 2 mole % KCl-CsCl molten mixture was similar to the above during heating. However, a rapid change in expansion is seen as the mixture cools from $250\text{-}200^\circ\text{C}$ which represents the range in which a solid-phase transition peak appeared in the DTA thermogram on cooling (Fig. 3).

When the KCl content was increased to 7 mole %, the temperature range of rapid expansion in the heating process shifted to 450-525°C (mechanical mixture). An abrupt contraction, however, took place between 200-250°C (compare with Fig. 4). With the molten mixture, this range further changed to 400-450°C. The temperature rate of expansion of the same mixture in the cooling step appeared to be quite uniform. However, there was a tendency for the pellet of this mixture (molten, 7 mole % KCl) to contract rather than expand in the heating step in certain temperature ranges.

Table 2. Thermal Expansion Characteristics of CsCl and KCl-CsCl Mixtures

| | Linear Expansion ^a (% of starting length ^b) | | | | | | Residual Expansion at Room Temp ^c |
|--|--|--------------|--------------|----------------|--------------|--------------|--|
| | On Heating to: | | | On Cooling to: | | | |
| | | | | | | | |
| <u>Pure CsCl</u> | <u>450°C</u> | <u>500°C</u> | <u>550°C</u> | <u>450°C</u> | <u>400°C</u> | <u>350°C</u> | |
| Cycle 1 ^d | 2.48 | 7.42 | 12.02 | 11.62 | 10.61 | 9.76 | 9.50 |
| Cycle 2 | 1.44 | 4.02 | 4.88 | 4.74 | 3.81 | 3.61 | 3.12 |
| Cycle 3 | 1.32 | 2.85 | 4.20 | 3.60 | 2.05 | 1.65 | f |
| <u>2 Mole % KCl-CsCl (Mech. Mixture)</u> | <u>450°C</u> | <u>500°C</u> | <u>550°C</u> | <u>400°C</u> | <u>350°C</u> | <u>300°C</u> | |
| Cycle 1 ^d | 2.84 | 3.46 | 6.56 | e | e | 9.30 | 8.68 |
| Cycle 2 | 1.66 | 5.53 | 5.63 | 4.35 | 3.38 | 2.90 | 1.46 |
| Cycle 3 | 1.80 | 3.05 | 3.80 | 3.16 | 2.70 | 2.43 | 1.53 |
| <u>2 Mole % KCl-CsCl (Molten)</u> | <u>400°C</u> | <u>450°C</u> | <u>500°C</u> | <u>300°C</u> | <u>250°C</u> | <u>200°C</u> | |
| Cycle 1 ^d | 3.34 | 5.03 | 9.02 | 7.89 | 7.14 | 5.08 | 4.83 |
| Cycle 2 | 1.14 | 1.69 | 4.42 | 3.10 | 2.42 | 0.78 | 0.73 |
| Cycle 3 | 1.20 | 1.83 | 4.58 | 2.94 | 2.68 | 0.96 | 0.77 |
| <u>7 Mole % KCl-CsCl (Mech. Mixture)</u> | <u>400°C</u> | <u>450°C</u> | <u>525°C</u> | <u>300°C</u> | <u>250°C</u> | <u>200°C</u> | |
| Cycle 1 ^d | 2.26 | 3.37 | 11.56 | 11.56 | 10.82 | 8.64 | 8.10 |
| Cycle 2 | 1.64 | 2.50 | 5.75 | 4.49 | 4.02 | 2.46 | 1.78 |
| Cycle 3 | 1.42 | 2.54 | 4.83 | 3.33 | 3.00 | 1.75 | 1.25 |
| <u>7 Mole % KCl-CsCl (Molten)</u> | <u>350°C</u> | <u>400°C</u> | <u>450°C</u> | <u>400°C</u> | <u>350°C</u> | <u>300°C</u> | |
| Cycle 1 ^d | 5.54 | 7.31 | 10.76 | 9.13 | 8.93 | 8.74 | 8.12 |
| Cycle 2 | -0.31 | 0.22 | 1.70 | -0.09 | -0.27 | -0.47 | f |

^aMeasurement made upon heating or cooling to the temperature indicated.

^bLength at the start of each cycle.

^cExpansion retained at the conclusion of each run.

^dOne cycle represents one heating-cooling cycle.

^eOut of scale.

^fPellet deformed; no measurement made.

B. Thermal Expansion Coefficient

The calculated result in Table 3 shows the variation in the coefficient of linear thermal expansion of the CsCl-KCl mixtures with the composition, the temperature range, and the previous history of the sample (e.g., whether

Table 3. Coefficient of Linear Thermal Expansion
for Pure CsCl and KCl-CsCl Mixtures

| Heating Cycle No. | Coefficient of Linear Thermal Expansion in Temperature Range ^a [in./ (in.·°C) × 10 ⁵] | | |
|----------------------|---|--------------------------|--------------------------|
| | <u>Pure CsCl</u> | | |
| 1 | <u>150-300°C</u> 6.06 | <u>300-480°C</u> 9.73 | <u>480-550°C</u> 240 |
| 2 | <u>150-400°C</u> 5.74 | | <u>475-550°C</u> 112 |
| 3 | <u>150-400°C</u> 4.92 | | <u>485-550°C</u> 104 |
| | <u>2 Mole % (or 0.9 wt %) KCl-CsCl (Molten)</u> | | |
| 1 | <u>100-250°C</u> 4.05 | <u>350-400°C</u> 13.1 | <u>450-500°C</u> 80.5 |
| 2 | <u>150-400°C</u> 4.42 | | <u>450-500°C</u> 55.4 |
| 3 | <u>100-350°C</u> 4.72 | | <u>450-500°C</u> 55.7 |
| | <u>2 Mole % (or 0.9 wt %) KCl-CsCl (Mechanical Mixture)</u> | | |
| 1 | <u>50-150°C</u> 5.94 | <u>200-400°C</u> 6.76 | <u>500-550°C</u> 62.7 |
| 2 | <u>100-400°C</u> 5.39 | | <u>450-500°C</u> 78.0 |
| 3 | <u>100-400°C</u> 4.96 | | <u>470-520°C</u> 34.3 |
| | <u>7 Mole % (or 3.2 wt %) KCl-CsCl (Molten)</u> | | |
| 1 | <u>100-150°C</u> 4.42 | <u>150-200°C</u> 10.4 | <u>200-250°C</u> 61.7 |
| 2 | <u>100-250°C</u> 2.18 | | <u>400-450°C</u> 30.2 |
| | <u>7 Mole % (or 3.2 wt %) KCl-CsCl (Mechanical Mixture)</u> | | |
| 1 | <u>100-400°C</u> 7.67 | <u>400-450°C</u> 22.9 | <u>450-535°C</u> 109 |
| 2 | <u>100-375°C</u> 4.74 | <u>400-450°C</u> 18.0 | <u>450-525°C</u> 43.4 |
| 3 | <u>100-380°C</u> 4.38 | <u>400-450°C</u> 23.2 | <u>450-500°C</u> 37.0 |

^aThermal expansion characteristics in the temperature ranges not indicated are rather complex.

sample was previously molten or not and the number of heating-cooling cycles). The coefficient after the solid-phase transformation was always considerably higher than that before transformation. Likewise, the mechanical mixtures exhibited higher expansion coefficients than the molten mixtures in the low temperature range. For example, for pure CsCl, the coefficient above the transformation point (464°C) was found to be approximately 20-40 times greater than that below the transition. An addition of a small amount of KCl (e.g., 2 mole %) reduced this difference drastically, but there still was a dramatic change (12 to 20 fold) in the expansion coefficient as the material was heated through the transition temperature range. The presence of KCl (up to 7 mole %) also tended to reduce the absolute value of the coefficient considerably. In all cases, the behavior of the material (cylindrical pellet) in the first cycle was rather complex presumably due to the thermal equilibration (annealing) effect. Except for the molten mixture of 2 mole % KCl-CsCl in the low temperature range, the coefficient tended to diminish with the number of heating-cooling cycles.

V. Phase Diagram of CsCl-KCl System

The phase diagram for the CsCl-KCl system depicted in Fig. 12 is based on the experimental results from the present study. The major source of data for the solidus and liquidus was the differential thermal analysis, while data for the solid-phase region was determined primarily from high-temperature x-ray diffraction analysis. The solidus and liquidus almost merge at the minimum temperature of about 600°C (liquidus at 596°C and solidus at 600°C) for a mixture containing approximately 35 mole % KCl. The solidus is nearly parallel to the abscissa in the composition range from 25 to 50 mole % KCl.

The presence of a continuous series of solid solution of CsCl and KCl in the region immediately below the solidus ($<600^{\circ}\text{C}$) was confirmed by high-temperature x-ray diffraction analysis. The approximate linear relationship between the lattice parameter and the KCl content shown in Fig. 13 for the β -phase quenched to room temperature in a dry atmosphere is additional support for the theory of continuous solution. This is based on Vegard's law stating that the lattice parameter of a continuous solid solution of ionic salts is directly proportional to the solute content. Evidence of two solid solutions of β_1 - and β_2 -phases having the same NaCl structure but different compositions and slightly different lattice parameters [e.g., see Fig. 6B-(2)] was also found. X-ray results likewise suggested the existence and approximate location of the monotectoid loop, although further experimental work will be required to establish a more precise shape of the loop in the high KCl range (the broken curve portion).

The monotectoid reaction takes place at about 28 mole % KCl and 360°C , decomposing the β -phase into the CsCl-rich α -phase and the KCl-rich β_2 -phase precipitates [also see Fig. 9(a) and (b)]. The solubility of KCl in CsCl is estimated to be 8 mole % at 360°C , while that of CsCl in KCl is less than 5 mole % at the same temperature. The solubility of KCl drops to about 5 mole % at 285°C .

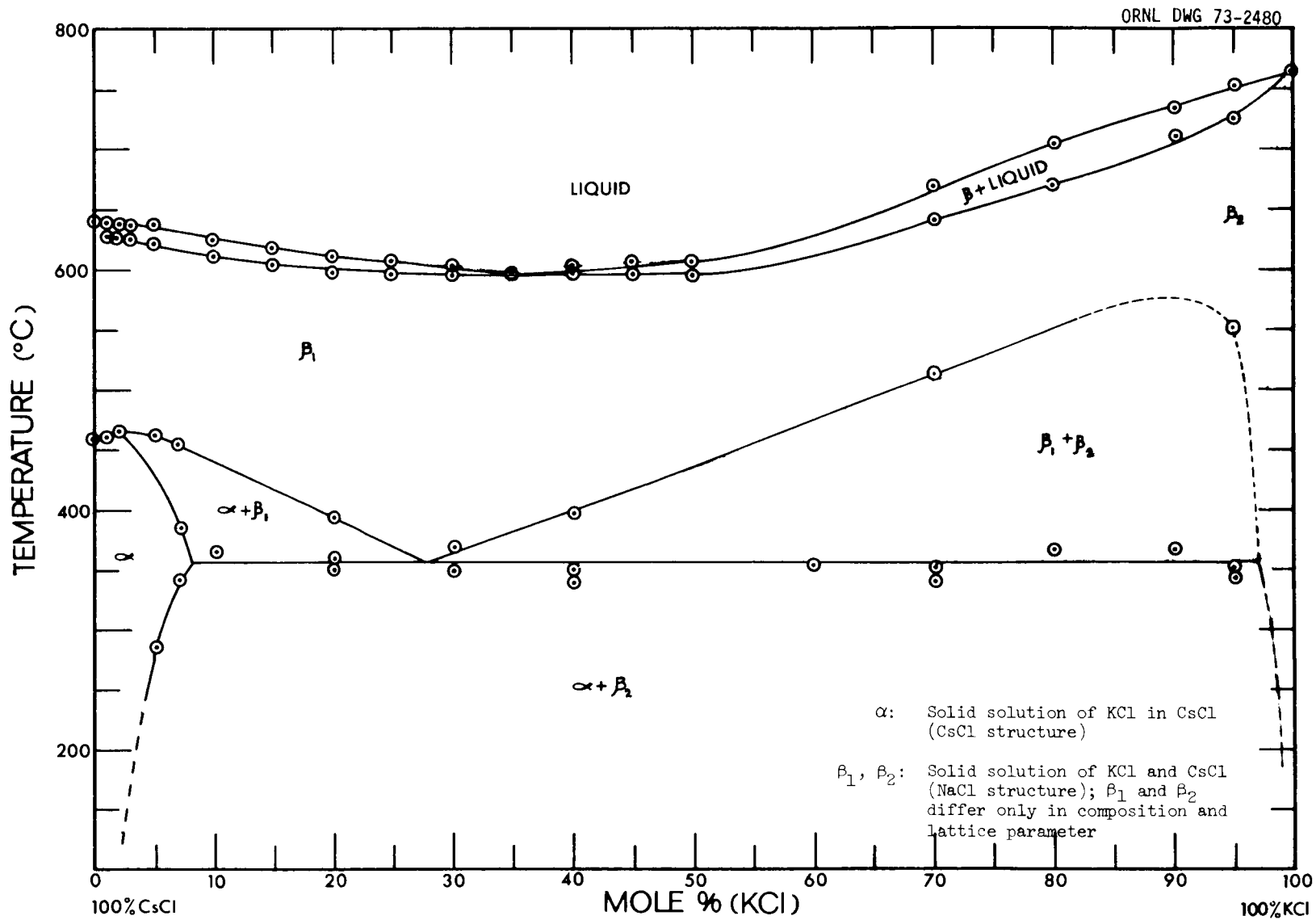


Fig. 12. Phase Diagram of CsCl-KCl System.

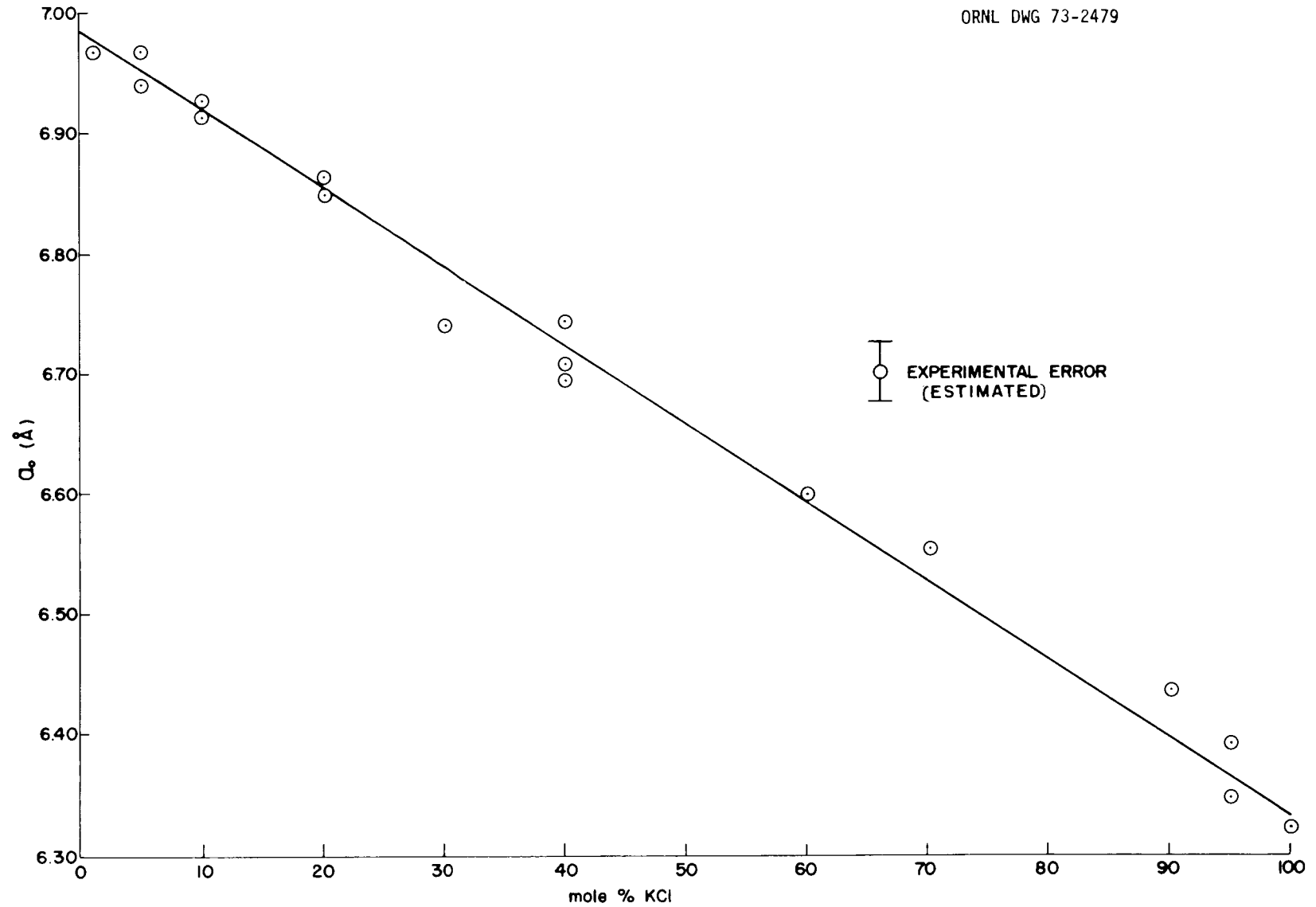


Fig. 13. Lattice Parameter a_0 of β -Phase as a Function of Mole % KCl in CsCl-KCl System (room temperature).

VI. Kinetics of Solid-Phase Transformation

The foregoing discussion dealing with the results from various experimental techniques suggests that the kinetics and mechanism of the $\alpha \rightleftharpoons \beta$ phase transformation in the KCl-CsCl system are influenced by the composition of the mixture, the isothermal annealing temperature (below transformation temperature of CsCl, 464°C), and the gaseous atmosphere surrounding the sample.

As illustrated in Fig. 14, the amount of β -phase retained at room temperature (after one thermal cycle through melting point) in a dry argon atmosphere increases with the increasing KCl content (up to 20 mole %), reaching the maximum of 100% near 20 mole % KCl. The percent β -phase retained was computed by subtracting the α (110) peak from 100% (i.e., the "single-line" technique). Although this technique is not precise, the calculated results (Fig. 14) adequately demonstrate that the $\beta \rightarrow \alpha$ or $\beta_1 \rightarrow \alpha + \beta_2$ phase transformation becomes more and more sluggish as increasing amounts of KCl are introduced in CsCl (up to approximately 15 mole % KCl). Above 15 mole % KCl, no $\beta_1 \rightarrow \alpha + \beta_2$ phase transformation

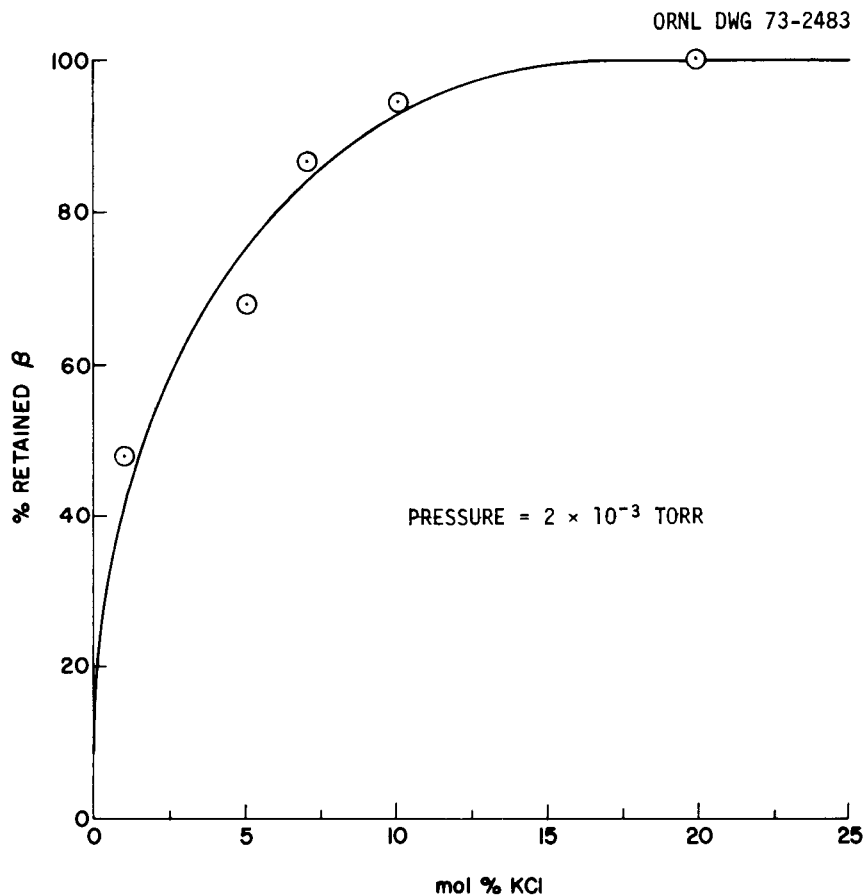


Fig. 14. Amount of β -Phase Retained in CsCl-KCl System at Room Temperature After One Thermal Cycling. (Argon Atmosphere)

was observed for an extended period of time (~ 10 hr for 20 mole % KCl-CsCl). Since the single-line x-ray diffraction analysis requires a diffracted intensity value from the pure phase, the 20 mole % KCl-CsCl was selected to investigate the roles of the annealing temperature and the gaseous atmosphere (specifically, the moisture) in the kinetics and mechanism of the transformation.

A. The $\beta_1 \rightarrow \alpha + \beta_2$ Phase Transformation in "Dry" Atmosphere

Shown in Fig. 15 are the rate curves depicting the amounts of β_1 -phase retained at different time intervals with annealing temperature as the parameter (pressure: 2×10^{-3} Torr). The transformation proceeded very slowly at room temperature (25°C), still retaining approximately 40% of β_1 -phase even after 600 hr. At 100°C , the rate of transformation is only slightly greater, but a dramatic increase in the rate was noted at 150°C . When the temperature was raised to 200°C , however, the increase in the rate was hardly noticeable, and, above this temperature, it began to decline significantly (see curves for 250 and 300°C).

Behavior of the 20 mole % KCl-CsCl can be explained based on the classical theory of heterogeneous nucleation stating that the rate of transformation is low near the transformation temperature and in the low-temperature range, reaching a maximum at some intermediate temperature (e.g., see ref. 6). Further discussion on this subject is presented in Section VII-C. Results similar to those above were obtained in several experiments using argon gas. However, use of the vacuum environment ($\sim 2 \times 10^{-3}$ Torr pressure) was maintained in this series of experiments in order to minimize the possibility of introducing moisture into the sample chamber and obscuring the influence of the annealing temperature.

B. The $\beta_1 \rightarrow \alpha + \beta_2$ Phase Transformation in Air

Figure 16 in combination with Fig. 15 demonstrates how the phase transformation was accelerated in air of 40% relative humidity. For example, the transformation was completed in 20 sec at 18°C , which is nearly 10^5 times faster than that in vacuum or argon gas. Higher annealing temperatures up to approximately 100°C appeared to retard the transformation rate. This behavior can be attributed to the diminishing amount of water vapor adsorbed onto the solid surface with increasing temperature. There are evidences that adsorbed water molecules exert a significant influence on the surface ionic conductance of the salt which, in turn, controls the rate of phase transformation (see Section VII-B for detail). The fact that the rate of transformation reversed the above trend with respect to temperature at 200°C presumably implies that the thermal effect is predominating the overall process at this temperature.

It should be pointed out that the technique employed in obtaining the data in Fig. 16 was a modification of that previously described (Experimental, Section II-E). Since the original technique of evaluating the integrated intensity (area under the peak) was too slow to record the rapid phase transformation

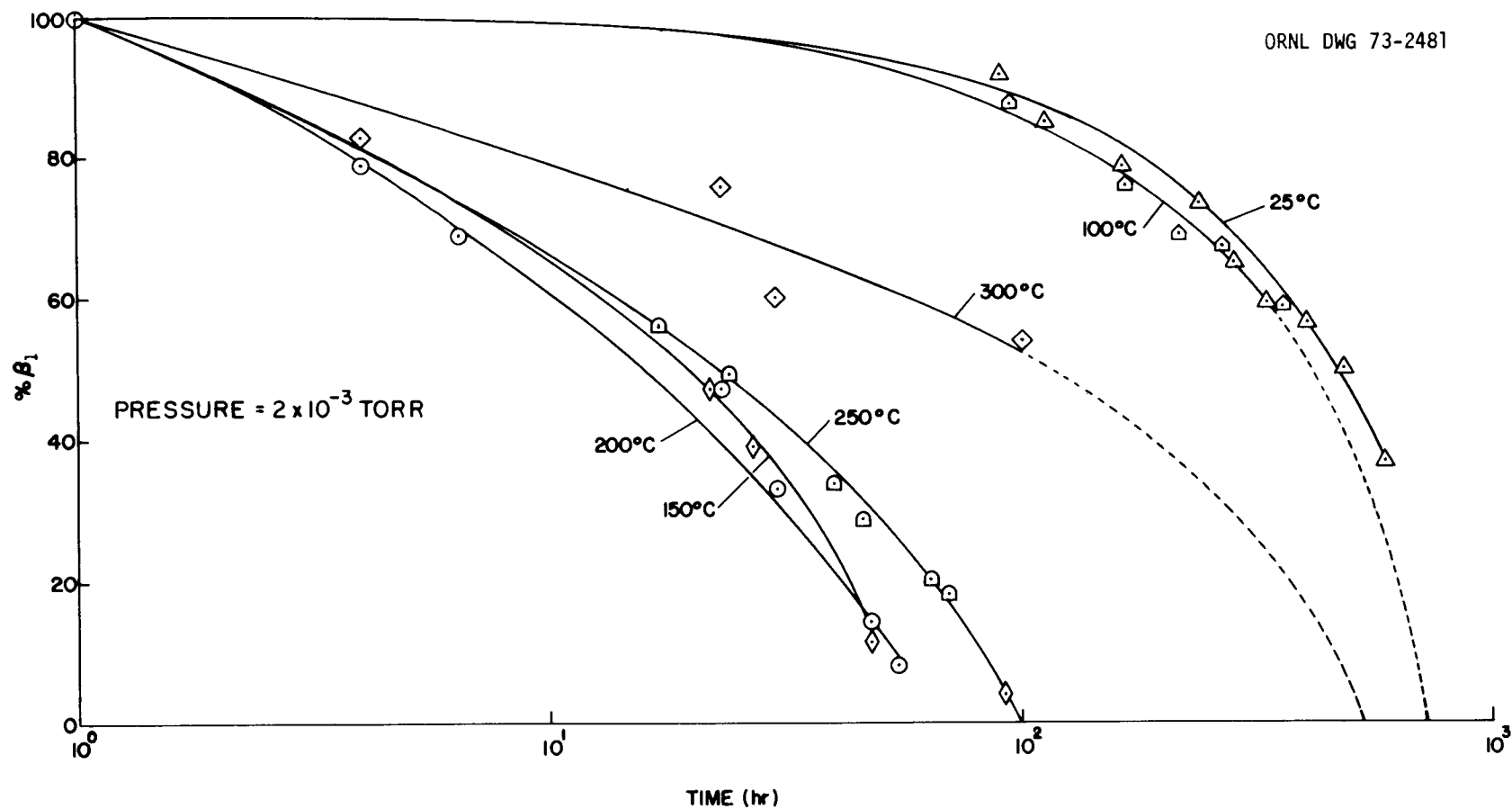


Fig. 15. Amount of β_1 -Phase Retained in 20 Mole % KCl-CsCl at Various Time Intervals and Annealing Temperatures.

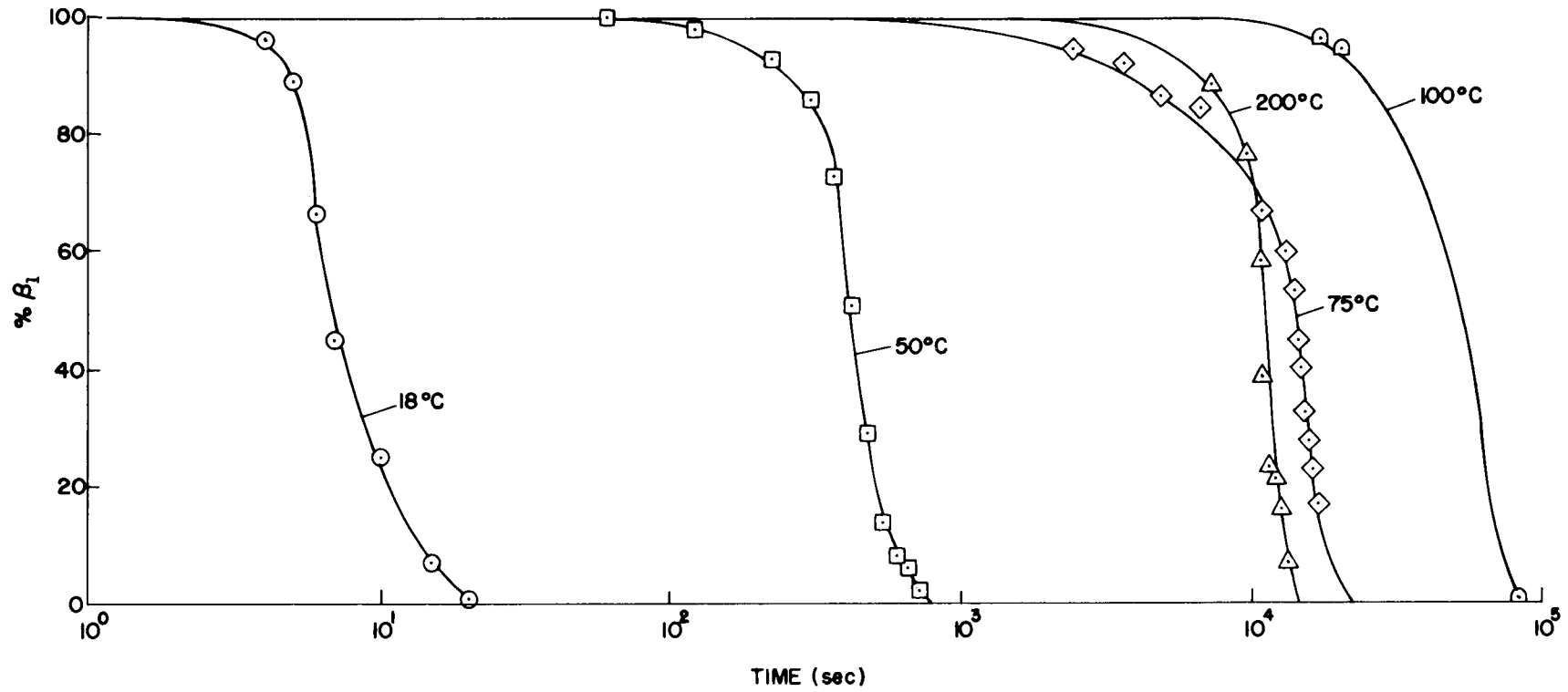


Fig. 16. Amount of β_1 -Phase Retained in 20 Mole % KCl-CsCl at Various Time Intervals and Annealing Temperatures (in air with 40% relative humidity).

in the presence of water vapor, the diffractometer was positioned to measure the maximum (peak) intensity of the β_1 (200) reflection. As soon as air was admitted to the sample chamber, the recorder was started, and the decay of the β_1 (200) peak was recorded directly against time. The normalized β_1 (200) decay was assumed to represent the percent β_1 -phase in the sample. Because the maximum intensity of β_1 (200) is probably not directly proportional to the amount of β_1 -phase present, the data obtained in this manner are not as accurate as those obtained from the integrated intensity. Nevertheless, the above technique is perhaps as good as or better than other techniques (e.g., photomicrographs), under the circumstances.

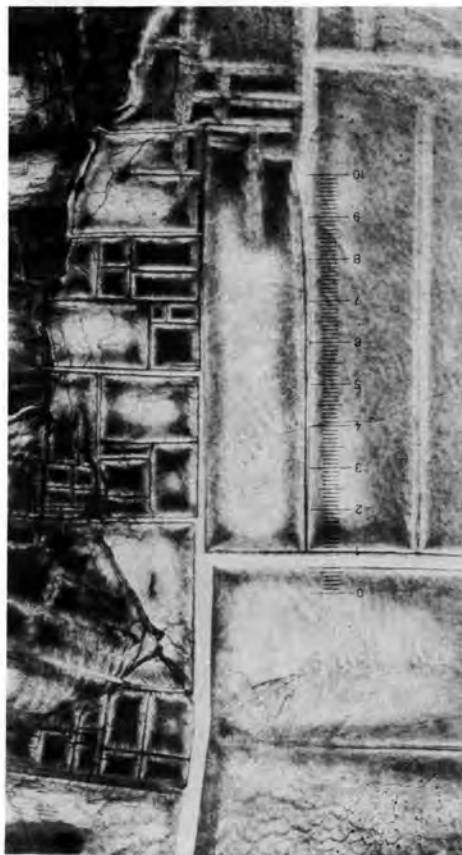
C. Observation Under Optical Microscope

The $\beta_1 \rightarrow \alpha + \beta_2$ phase transformation was also observed visually using a high-temperature metallograph. The results of these experiments are illustrated by the photomicrographs in Fig. 17. Figure 17a shows a portion of 20% KCl + CsCl which was cooled from the melt under argon and is composed entirely of the β_1 -phase. The rectangular fractures were formed because of thermal contraction during cooling and are probably oriented along (100) faces of the cubic structure. Figure 17b shows the same area 2 min after the quartz cover glass was removed, exposing the β_1 -phase to air. The dark areas are presumably portions of the β_1 -phase solid solution which have transformed to the α - and β_2 -phases. The transformation seems to be nucleated at exposed surfaces since thin areas and crystal edges darkened first. Shown in Fig. 17c is the sample 4 min after exposure to air. The $\beta_1 \rightarrow \alpha + \beta_2$ phase transformation appears nearly complete, and the crystals are almost opaque. The crystals in the field of view are not uniformly dark because of the difference in sample thicknesses at various locations.

The light areas in the upper right hand corner were very thin, while the darker areas in the center and to the left were about four to five times thicker. The $\beta_1 \rightarrow \alpha + \beta_2$ phase transformation shown in Fig. 17 took approximately 4 min, while the x-ray data in Fig. 16 show that the transformation at 18°C took only 20 sec. This apparent discrepancy can be explained as follows. Argon gas in the sample chamber of the microscope is considerably heavier than either air or water vapor. Accordingly, it took much longer for water vapor to diffuse to the solid surface by natural convection than in the case involving the x-ray diffraction sample in which air was introduced into an evacuated chamber ($\sim 2 \times 10^{-3}$ Torr pressure) under flowing condition. Observation under the microscope was facilitated by such a gradual transformation.



(a) 20°C; Argon atmosphere



(b) 20°C; 2 min after exposure to air



(c) 20°C; 4 min after exposure to air

Fig. 17. Solid-Phase Transformation of 20 Mole % KCl-CsCl Upon Exposure to Air (40% relative humidity). Magnification: 125X.

VII. Assessment of Consolidated Results

The experimental results presented thus far disclosed the complex behavior of CsCl in the structural transformation in the presence of KCl. The rate and the type ($\alpha \rightleftharpoons \beta$ or $\alpha + \beta_1 \rightleftharpoons \beta_2$) of the solid-phase transformation were found to depend upon a number of parameters including the composition, temperature, and the presence or absence of water vapor in the gaseous atmosphere. The rate was also governed by whether it was in the cooling or heating step. An attempt is made below to elucidate this seemingly anomalous behavior of the CsCl-KCl system.

A. Role of KCl

Electrical conduction by ions in a solid is generally the result of lattice imperfections (defects). Variation in the ionic conductivity of ionic crystals with the impurity content as well as temperature is well known. The influence of impurities usually stems from size and charge effects. There are evidences to show that the presence of KCl in CsCl exerts pronounced effects on the ionic conductivity and other properties associated with solid-phase transformation.

The activation energy of diffusion, E , is related to the ionic conductivity, ω , by the following expression:

$$\omega = (A/T) \exp(-E/kT) \quad (1)$$

where k is the Boltzmann constant, A the pre-exponential factor, and T is the temperature. The activation energy, in turn, is made up of two energy terms, namely, the energy of formation of a Schottky defect (E_f) and the migration energy barrier (E_m) as in:

$$E = E_m + 1/2 E_f \quad (2)$$

In general, E_m can be described by:⁷

$$E_m = C_1 k_s [r^+ - r_i + (1-C_2)r_o]^2 \quad (3)*$$

Here, C_1 is a correction factor to account for deviation of ions from hard spheres, C_2 is a constant, k_s represents the Einstein spring constant, r^+ and r_i are the radii of the host ion and the impurity ion, respectively, and r_o is the nearest-neighbor distance. On the other hand, E_f consists of the static lattice energy per pair of ions (E_l) and the energy change at the time when the defect is formed (E_r) as in:

$$E_f = E_l - E_r \quad (4)*$$

*See ref. 7 for details on the theory and assumptions leading to Eqs. (3) and (4) and the expression for E_r including the static dielectric constant.

With a rising temperature, the ionic conductivity of CsCl increases continuously until the solid-phase transformation temperature is reached, when an abrupt drop in the conductivity (from about 10^{-4} to 10^{-6} mho/cm) occurs. An upward trend in the conductivity resumes upon completion of the transformation from the low-temperature (CsCl) structure to the high-temperature (NaCl) structure. According to the experimental results of Harvey and Hoodless⁸ in the determination of ionic conductivity and diffusion coefficient, the anion is the major current carrier in pure CsCl. The contribution of cations to the ionic conductivity is enhanced remarkably by introduction of cations having ionic radii smaller than the Cs⁺ ion⁹ (e.g., K⁺ and Rb⁺). For example, the ionic conductivity of single crystals of CsCl doped with 5 atom % of K⁺ increased by approximately 65% over that of pure CsCl at 597°C (2.3×10^{-5} mho/cm vs 1.4×10^{-5} mho/cm). Such an increase in the conductivity is presumably attributable to the lower value of E_m (migration energy barrier) for K⁺ ions than that for Cs⁺ ions in mixed crystals. The E_m values calculated⁹ from Eq. (3) for Cs⁺ and K⁺ ions are respectively 0.73 and 0.17 eV in the low-temperature range (CsCl structure) and 1.3 and 0.35 eV in the high-temperature range (NaCl structure). Thus, K⁺ ions are major current carriers in the mixed crystals of CsCl and KCl.

The role of K⁺ ions in the ionic conductivity of the CsCl-KCl system is reflected on other properties. For example, the solid-phase transformation temperature of the system on heating declines as the KCl content is increased⁹ (up to 5 mole %). Similarly, both the activation energy (E) and the pre-exponential factor (A) diminish with increasing KCl content. An increase in the amount of KCl likewise reduces the enthalpy of solid-phase transformation (ΔH), which becomes zero at approximately 9 mole % KCl.¹⁰ On the other hand, the width of hysteresis (the difference between the transformation temperature on heating and that on cooling) is proportional to the KCl content up to about 5%.

The reduction in ΔH with an increase in the KCl content explains the diminishing transformation peak in the DTA thermogram (Figs. 1 through 5). In addition, the decrease in the activation energy of diffusion (E) probably implies an increase in the speed of transformation, resulting in disappearance of the peak on heating the mixture containing more than 2 mole % of KCl. That is, the change in the sample temperature caused by the small ΔH may not have been detected due to rapidity of the transformation. The sluggish transformation behavior in the cooling step might be attributable to the reconstructive transformation¹¹ of the system in the presence of the impurity KCl that has the structure (NaCl) different from the low-temperature structure of CsCl. Thus, in changing the first coordination (relation between the nearest-neighbor atoms) on cooling, the system presumably had to go through an intermediate coordination which acted as a barrier to the transformation. The phenomena of declining transformation temperature and increasing width of hysteresis mentioned above also agree with observations in the DTA and x-ray diffraction studies.

B. Effect of Moisture

Water is a polar solvent with a high dielectric constant. Because of their electrolytic characteristic, water molecules possess strong attractions for ions and tend to dislodge them from their positions in the crystal lattice to produce solvated ions. In ionic crystals (e.g., alkali halides), ionic conduction results from the movement of lattice defects under the influence of an electric field. Consequently, the conductivity of the ionic crystals is expected to be influenced by moisture in the gaseous environment surrounding the crystals.

Such an effect of moisture on the ionic conductivity was demonstrated by the experiments of Oberlin and Hucher¹² who established curves correlating the surface conductance (log scale) with the partial pressure of water vapor for NaCl, KCl, NaBr, and KBr. All of the curves exhibited two points of inflection, the locations of which varied with individual salts. A comparison of these curves with the morphology of cleavage face (as shown by electron micrographs) revealed that the sudden increase in the density of spot-like formation took place immediately after the first point of inflection. This point represented formation of the first monolayer and hydration of lattice ions. When the partial pressure of water was increased beyond the second point of inflection, the spot-like formation began to disappear, but spots became localized in "domains." This phenomenon was attributable to the onset of dissolution. Changes in the surface structure (due to recrystallization) of thin films of alkali halides upon exposure to atmospheric moisture have been observed under the electron microscope by several authors.¹³⁻¹⁵

The dramatic effect of moisture on the solid-phase transformation of the CsCl-KCl system in the cooling step has already been discussed (Section VI-B; Figs. 15 and 16). For the 20 mole % KCl-CsCl sample, the $\beta_1 \rightarrow \alpha + \beta_2$ phase transformation at room temperature in moist air (40% relative humidity) was nearly 10^5 times faster than that in a dry atmosphere (argon or $\sim 2 \times 10^{-3}$ Torr pressure). The acceleration of the transformation mentioned above is most likely the result of a sudden increase in ionic conductivity due to moisture, which facilitated the transformation. This assumption is based on the foregoing discussion in regard to the variation of ionic conductivity of alkali halides with moisture and with KCl content.

C. Temperature Effect

When a solid phase is in a metastable state, thermally activated fluctuations may produce nuclei for transformation to a more stable solid phase. According to the classical theory of nucleation,⁶ the rate of nuclei formation under steady-state conditions per unit volume of the parent phase is described by:

$$\gamma_n = A_n \exp[-(E_n + \Delta G_{\max})/kT] \quad (5)$$

where E_n is the activation energy controlling the rate of interface movement, A_n^n represents the pre-exponential factor, ΔG_{\max} is the maximum free energy of formation of embryos (spherical) of a critical nucleus size (r_c), k is the Boltzmann constant, and T is the absolute temperature.

It can be shown from the theory⁶ that the free energy of formation of embryo (ΔG) varies with the nucleus size (r) and temperature. Both ΔG_{\max} and r_c also depend upon temperature. As the temperature approaches that of the equilibrium transformation, ΔG_{\max} increases rapidly, implying that the nucleation rate will be very low [see Eq. (5)]. Likewise, the nucleation process is expected to be slow at low temperatures. Assuming that the rate of solid-phase transformation under the isothermal condition is governed directly by the initial rate of nucleation, the above discussion leads to a prediction that the rate of transformation will diminish at low temperatures and near the transformation temperature. That is, the rate will be a maximum at an intermediate temperature. The qualitative reasoning presented above explains the behavior of the CsCl-KCl system in a dry atmosphere at different annealing temperatures (e.g., see Section VI-A; Fig. 15). For example, the $\beta_1 \rightarrow \alpha + \beta_2$ phase transformation of the 20 mole % KCl-CsCl (equilibrium transformation temperature $\cong 360^\circ\text{C}$) was quite slow at room temperature (i.e., only 60% complete after 600 hr). The rate increased continuously as the annealing temperature was raised successively to 200°C . Further increase beyond this temperature made the rate drop sharply.

The kinetic behavior of the type described in the preceding sections has also been observed in the solid-phase transformation of a number of metals and alloys, including low alloy steels. Such behavior can be represented by a series of "C"-shaped curves, shown in Fig. 18* for 20 mole % KCl-CsCl, when a plot is made of the reciprocal of annealing temperature (linear scale) versus the time required for transformation of certain fraction of β -phase (log scale). The nose of the C curve corresponds to the maximum transformation rate. The fact that the kinetic behavior of the 20 mole % KCl-CsCl follows the trend of the C curve implies qualitatively that the solid-phase transformation of this mixture can be approximated by the mechanism based on the classical theory of homogeneous nucleation.

*If more than one solid-phase transformation is involved, there will be several individual series of C curves (one for each transformation) arranged in the order of increasing or decreasing temperature range.¹⁶

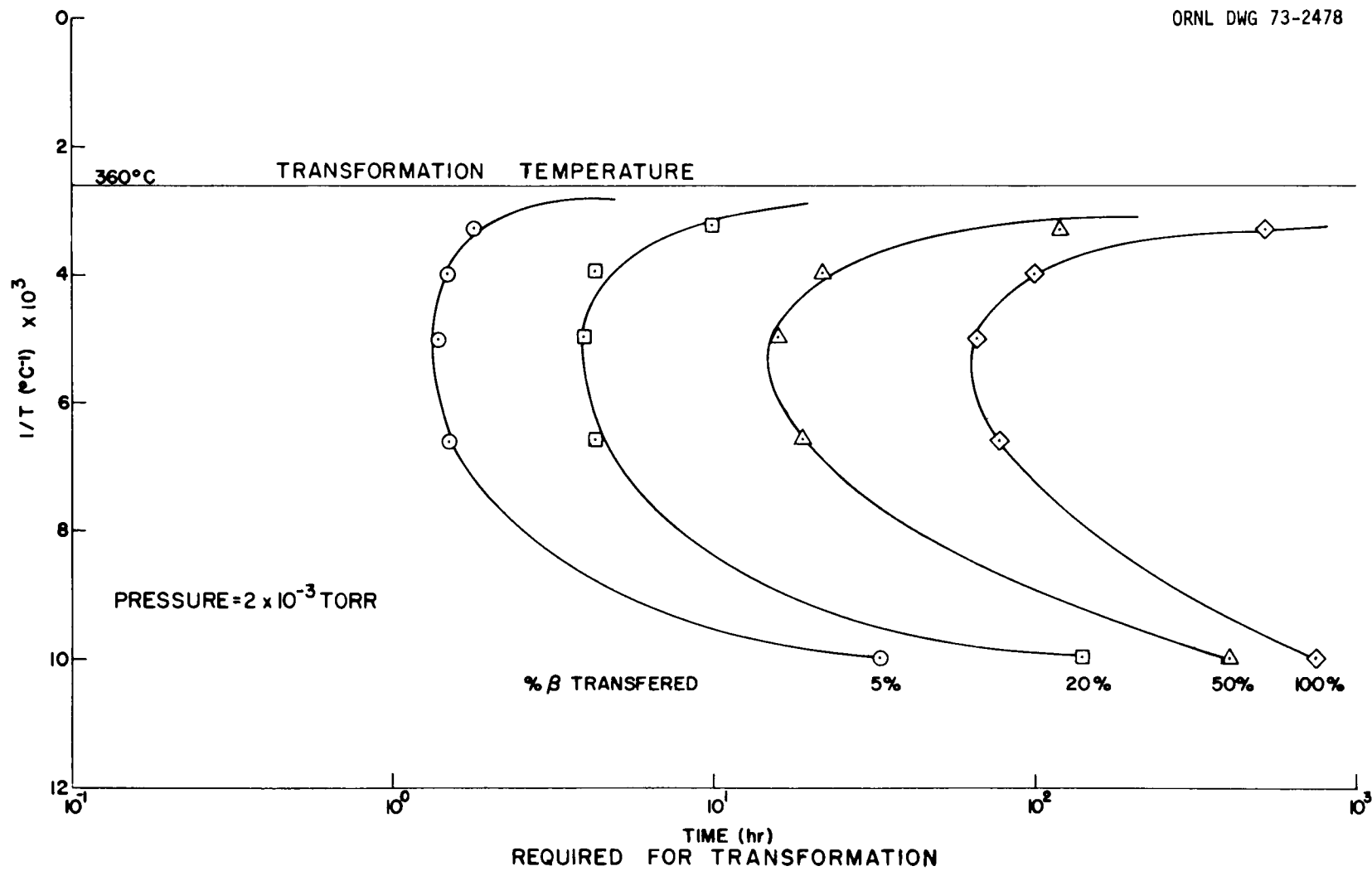


Fig. 18. Isothermal Time-Temperature-Transformation Diagram for 20 Mole % KCl-CsCl.

CONCLUSIONS AND RECOMMENDATIONS

In the presence of potassium chloride, cesium chloride displays complex behavior with regard to solid-phase transformation and the resultant thermal expansion. Differential thermal analysis is not capable of detecting the full extent of such a complex behavior, and results tend to be misleading. The shrinking transformation peak area and eventual disappearance of the peak on the DTA thermogram for the CsCl-KCl mixtures with greater than 2 mole % KCl are attributable to the diminishing amount of heat of transformation with increasing KCl content. The sluggish transformation in the cooling step in a dry atmosphere is possibly due to the reconstructive nature of the transformation in the presence of KCl.

Despite such a confusing behavior, the solid-phase transformation does take place in the CsCl-KCl system as verified by the results from dilatometry and from high-temperature x-ray diffraction analysis and metallography. At low concentrations of KCl (<5 mole %), the transformation temperature drops and the transformation hysteresis widens as KCl content is increased. Further increase in the KCl content renders the transformation behavior more involved. The roles of the composition and temperature in determining the type of transformation may be illustrated by a phase diagram that shows a monotectoid system in the solid-phase region. At high temperatures ($\sim 600^\circ\text{C}$) CsCl and KCl form a continuous solid solution at all compositions. The solid solution decomposes monotectoidally at 28 mole % KCl when cooled to approximately 360°C . The maximum solubility of KCl in CsCl is about 8 mole % at 360°C , while that of CsCl in KCl is less than 5 mole % at the same temperature.

The kinetics of solid-phase transformation of the CsCl-KCl system is influenced most remarkably by moisture in the gaseous environment, and, to a lesser extent, by the KCl content and temperature. The moisture effect was especially notable during isothermal annealing below the transformation temperature. The kinetic behavior of the system is presumably related to the ionic conductivity which has been shown by other investigators to vary considerably with moisture content as well as with KCl content and temperature. A dramatic effect of moisture was observed with the 20 mole % KCl-CsCl mixture in which the sluggish transformation, observed on cooling to room temperature in the dry environment, was accelerated by a factor of 10^5 when exposed to air of $\sim 40\%$ relative humidity. The rate of transformation of the same mixture during the cooling step in the dry atmosphere was slow in the low-temperature range and near the transformation temperature, but reached a maximum value at some intermediate temperature. Thus, the transformation in the cooling step appears to follow a mechanism based on the classical theory of homogeneous nucleation.

The thermal expansion behavior of the CsCl-KCl system (up to 7 mole % or 3.2 wt % KCl) is somewhat unique in that the system has a tendency to retain a significant amount of residual expansion at room temperature after thermal cycling. Also, a large difference exists in the coefficient

of linear expansion between the pretransformation and posttransformation conditions. The coefficient after transformation is always much greater than that before transformation. Both the amount of residual expansion and the difference in the expansion coefficients are the largest for pure CsCl. Incorporation of KCl in CsCl tends to moderate this behavior.

In view of these results, capsule design for the $^{137}\text{CsCl}$ gamma source must take into consideration the tendency of CsCl to retain residual thermal expansion when subjected to thermal cycling. Also the problem of a sudden increase in the volume at the point of solid-phase transformation must be considered. Likewise, in the application of the source, conditions that tend to increase the temperature beyond the transformation temperature or to induce thermal cycling should be minimized. The presence of a small amount of KCl (e.g., up to 2 mole % or 0.9 wt %) as an impurity may be beneficial from the viewpoint of reducing the amount of residual thermal expansion and moderating the drastic change in the coefficient of thermal expansion.

ACKNOWLEDGMENT

The authors wish to express their appreciation to T. D. Owings for his assistance in DTA and thermal expansion experiments.

REFERENCES

1. S. Zhemchuzhnui and F. Rambach, *Z. Anorg. Chem.* 65, 421 (1910).
2. O. S. Dombrovskaya, *Zh. Obshch. Khim.* 3(8), 1019 (1933).
3. I. I. Ilyasov and A. G. Bergman, *Russian J. Inorg. Chem.* 7(3), 355 (1962).
4. H. T. Fullam, *Physical Property Measurements on CsCl and CsCl-Alkali Metal Chloride Systems*, BNWL-B-74, Pacific Northwest Laboratory (March 1971).
5. B. D. Cullity, *Elements of X-Ray Diffraction*, Addison-Wesley Publishing Company, Inc., London, 1959, pp. 389-91.
6. J. Burke, *The Kinetics of Phase Transformation in Metals*, Pergamon Press, London, 1965.
7. J. G. Mullen, *Phys. Rev.* 143(2), 658-62 (1966).
8. P. J. Harvey and I. M. Hoodless, *Phil. Mag.* 16, 543 (1967).
9. J. Arends and H. Nijboer, *Phys. Stat. Sol.* 26, 537-42 (1968).
10. H. Weijma and J. Arends, *Phys. Stat. Sol.* 35, 205-10 (1969).
11. M. J. Buerger, *Phase Transformations in Solids*, Chapter 6, R. Smoluchowski (ed.), Wiley & Sons, London, 1951.
12. A. Oberlin and M. Hucher, *Coll. Intern. CNRS No. 152, Adsorption et Croissance Cristalline*, 407-17 (1965), CNRS édit.
13. T. A. McLauchlon, R. S. Sennett, and G. D. Scott, *Can. J. Res.* A28, 530 (1950).
14. J. A. Joebst, *International Congress for Electron Microscopy, 5th Philadelphia, Pa., 1962*, Vol. 1, S. S. Breese (ed.), pp. 6-11, Acad. Press, New York, 1962.
15. D. N. Braski, *J. Nucl. Instrum. Methods* 102, 553-66 (1972).
16. *Supplement to the Atlas of Isothermal Transformation Diagrams*, U. S. Steel Company, Pittsburgh, 1953.

ORNL-4872
UC-23 - Radioisotope and
Radiation Applications

INTERNAL DISTRIBUTION

- | | |
|-------------------------------------|-----------------------|
| 1-3. Central Research Library | 57. R. F. Hibbs |
| 4. ORNL - Y-12 Technical Library | 58. E. H. Kobisk |
| Document Reference Section | 59. E. Lamb |
| 5-24. Laboratory Records Department | 60-79. K. H. Lin |
| 25. Laboratory Records, ORNL R.C. | 80. J. P. Nichols |
| 26. P. S. Baker | 81. T. D. Owings |
| 27. E. E. Beauchamp | 82. M. E. Ramsey |
| 28. G. E. Boyd | 83-84. R. A. Robinson |
| 29-48. D. N. Braski | 85. A. F. Rupp |
| 49-51. T. A. Butler | 86. R. W. Schaich |
| 52. F. N. Case | 87. M. J. Skinner |
| 53. J. A. Cox | 88. D. B. Trauger |
| 54. F. L. Culler | 89. A. M. Weinberg |
| 55. D. E. Ferguson | 90. J. C. White |
| 56. J. H. Gillette | 91. A. Zucker |

EXTERNAL DISTRIBUTION

- 92. H. L. Atkins, Brookhaven National Laboratory, Upton, New York
- 93. R. F. Barker, AEC, Washington, D.C.
- 94. N. F. Barr, AEC, Washington, D.C.
- 95. G. L. Borsheim, ARHCO, Richland, Washington
- 96. T. D. Chikalla, PNL, Richland, Washington
- 97. D. F. Cope, AEC Site Representative, ORNL
- 98. E. E. Fowler, AEC, Washington, D.C.
- 99-101. J. H. Jarrett, PNL, Richland, Washington
- 102. J. E. Machurek, AEC, Washington, D.C.
- 103. J. N. Maddox, AEC, Washington, D.C.
- 104. J. C. Malaro, AEC, Washington, D.C.
- 105. B. Manowitz, Brookhaven National Laboratory, Upton, New York
- 106. L. A. Miller, AEC, Washington, D.C.
- 107. W. D. Sandberg, AEC, Aiken, South Carolina
- 108. Robert E. Smith, Atlantic Richfield Hanford Company, Richland, Washington
- 109-114. D. H. Turno, SRL, Aiken, South Carolina
- 115. Research and Technical Support Division, AEC, ORO
- 116. Patent Office, AEC, ORO
- 117-299. Given distribution as shown in TID-4500 under Radioisotope and Radiation Applications category (25 copies - NTIS)